

LASER-ULTRASONICS: PRINCIPLES AND INDUSTRIAL APPLICATIONS

Jean-Pierre Monchalain

*National Research Council of Canada
75, de Mortagne Blvd, Boucherville, Québec, J4B 6Y4, Canada*

A broad overview of the field of laser-ultrasonics is presented. This overview draws from developments at the National Research Council of Canada (NRC) as well as elsewhere. The principles of generation and detection are presented, stressing a few key characteristics of laser-ultrasonics: the material is actually the emitting transducer and transduction is made by light, thus eliminating any contact. These features carry both advantages and limitations that are explained. Another feature, which has been an impediment, is actually the complexity of the 'laser-ultrasonic transducer', but in spite of this complexity, it can be made very reliable for use in industrial environments. It also can be very cost effective for a number of applications and we present those currently used in industry: essentially, the inspection of polymer matrix composites used in aerospace, the thickness gauging of hot steel tubing in production and the measurement and characterization of thin layers in microelectronics by two different approaches. Technological aspects, such as interferometer design, detection lasers and others are also discussed, as well as digital processing and imaging methods adapted to the technique. Many applications that have been the object of laboratory experimentation, as well as those that have been demonstrated in industrial plants with prototype systems are also described. As an overall conclusion, laser-ultrasonics that was for a long time a laboratory curiosity has definitely now made its transition to industry. Being unique by combining the power of ultrasound sensing for characterizing materials and processes with sensitive non-contact transduction with lasers and optics, laser-ultrasonics is expected to find broader use within the Smart Industry or Industry 4.0 revolution.

1. Introduction

Laser-ultrasonics is a particular implementation of ultrasonic nondestructive inspection in which ultrasound is generated and detected by lasers. The piezoelectric transducer widely used in the usual or conventional inspection by ultrasound is replaced by a laser and optical system. Since ultrasound is at the basis of material testing like conventional ultrasonics, laser-ultrasonics entails the same applications, which include thickness measurement, flaw detection and material characterization. Thickness measurement is based on the measurement of the time interval between the entrance of the ultrasonic wave in the tested part and the return echo from the back wall of the part or the measurement of the time interval between successive echoes. Flaw detection and characterization is based on the interaction of ultrasound with the flaw, which appears either as a reflection signal, a modification of the ultrasonic wave transmission or a scattered signal. Material characterization is based on the interaction of ultrasound with material microstructure, which shows as a change of ultrasonic attenuation or ultrasonic velocity or the production of noise-like signals from scattering.

The generation of ultrasound with lasers actually nearly goes back to the invention of the first laser, the ruby laser ¹, which was used to generate ultrasound or shock waves in materials ^{2,3}. Optical detection has on the other hand developed more slowly, being for a long time limited to laboratory settings before practical means to implement it in industrial environment were devised. Due to this difficulty to provide sensitive and practical detection in industrial environments, generation has been sometimes coupled with conventional detection with piezoelectric transducers or detection with electromagnetic acoustic transducers (EMATs) or air-coupled transducers.



As shown in figure 1, a laser ultrasonic transducer has typically three basic elements, a generation laser, a detection laser and an interferometer, followed by data acquisition and processing electronic hardware. These elements are sketched in figure 1 next to those which compose conventional piezoelectric-based ultrasonics. The key features that make laser-ultrasonics unique and distinguishes it from conventional piezoelectric ultrasonics and encompass advantages as well as drawbacks are the following:

- Transduction (generation and detection) is performed by light, which insures completely non-contact operation, operation at a distance that could range from centimeters to meters and allows operation in vacuum. The distance between the transduction hardware and the tested part can be much larger in laser-ultrasonics than in other known non-contact means, such as EMATs or air-coupled transducers. EMATs require fairly closed proximity to the part, typically of the order of 1 mm or a couple of mm while the strong attenuation of ultrasonic waves in air strongly limits the offset distance from the part for air coupled-transducers. Laser-ultrasonics does not require an electrically conductive part like EMATs, which limits essentially their use to metals and could operate in vacuum or at reduced pressure, which not feasible with air-coupled transducers.
- The material is the emitting transducer. This distinguishes laser-ultrasonics from piezoelectric-based ultrasonics in which the source of ultrasound is a piezoelectric element separated from the tested material. Below, we will discuss of the various mechanisms that insure ultrasound generation. This is a key factor that provides fairly broad independence to part shape and orientation of the part surface with respect to the laser beam. The fact that ultrasound is emitted by the part itself has however the drawback that too high laser power or energy could cause undesirable damage. Also transduction efficiency could be highly variable since it depends upon the optical absorption properties.
- Detection is generally from the part surface and consists in sensing the motion of this surface produced by the ultrasonic wave (reflected by the back wall of the part or some inner discontinuity as sketched in figure 1). In the unusual case in which the surface is covered by a layer transparent to the detection laser beam, the motion of an inner surface could also contribute to the signal. As a consequence, sensitivity of the technique depends upon on the reflection properties of the surface. If the surface scatters light there will be a broad independence from the direction of incident laser beam. Otherwise in the case of a shiny or mirror-like surface a strong signal will be only observed when the detection beam is sent essentially normal to the surface.
- Optics has the flexibility to provide generation and detection spots with very various shapes (small point, disk, circle, line, array of lines ..) and size appropriate to maximize a wave type and sensitivity.
- Laser-ultrasonics usually allows testing over a wide range of frequencies in comparison to piezoelectric transduction which is based on an electrically excited mechanical oscillator which could only give short pulses and high frequencies by damping the oscillation. By opposition in laser-ultrasonics the range of ultrasonic frequencies could be very high since very short ultrasonic pulses can be obtained by using short pulse generation lasers. GHz frequencies can be easily obtained. In the other hand of the spectrum, since there is no mechanism to cause oscillation, the displacement or the force at the source is unipolar and has a spectrum starting from zero frequency, which will be only cut to some value around 1 MHz or below by the detection interferometer.

- Generation mechanism does not generally allow selecting a wave type: longitudinal, shear and surface waves (or plate waves) are generally all emitted at the same time, which is depending upon the application a benefit or a drawback.
- The implementation equivalent to multi-element transducer to get a phase-array is certainly possible but will be complex, not practical, as well being costly, if it is done in real time. We will explain below that it is possible to get the equivalent of phase-array by numerical processing an array of previously acquired laser ultrasonic signals.
- Repetition rate of the same order as piezoelectric conventional ultrasonics, which ranges up to several kHz and is readily obtained by electronic pulse generators is possible, but is in the present state of laser technology and in view of the energies required for many applications will tend to be costly.
- Ultrasonic generation with lasers usually produce waves in the elastic regime of the same magnitude as piezoelectric transducers, but in the case in which generation is produced by a constrained plasma very strong waves (shock waves) can be produced. In this case nonlinear effects, plastic deformation and material breakage can be produced.

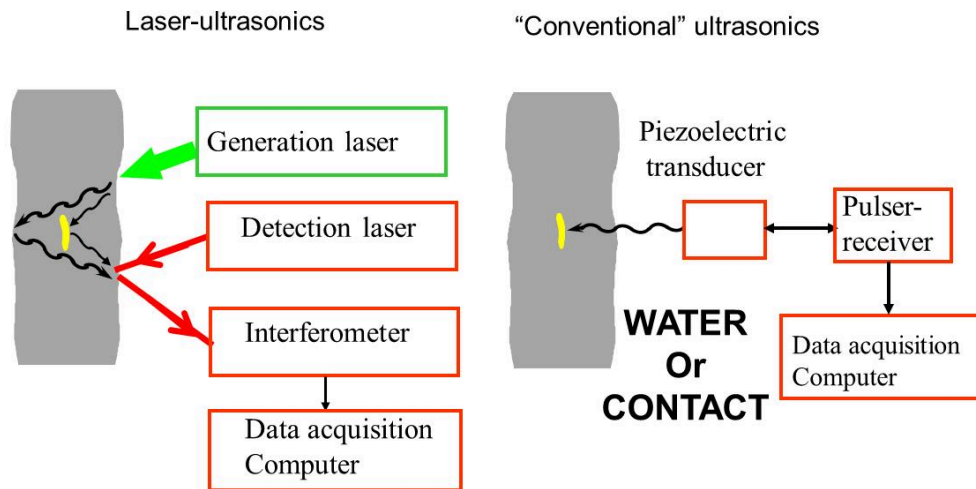


Figure 1. Sketch of the principle of laser-ultrasonics or of a “laser-ultrasonic transducer” compared to conventional piezoelectric-based ultrasonics.

2. Laser Generation of Ultrasound

There are essentially two kinds of mechanisms for generating ultrasound, the first one is perfectly nondestructive and is based on a thermoelastic mechanism (see figure 2) while the second one is invasive and is based on the ablation of the sample or on the vaporization of some surface layer.

2.1 Thermoelastic generation

The principle is the following: laser light is absorbed to some depth inside the material releasing heat locally; the heated region then expands producing a strain and a corresponding stress that is the source of waves propagating in the material or at its surface. Each heated point inside the material is a center of expansion to which 3 orthogonal force dipoles can be associated ^{4,5}. When the surface is free and when light penetration is very small compared to the acoustic wavelength (which is often the case in metals), the dipole normal to the surface cancels leaving only the in-plane dipoles. This situation has been extensively studied theoretically and experimentally ⁴⁻⁸. In the near field, the displacement signal appearing on the opposite surface of a plate sample consists of a first depression step corresponding to the longitudinal wave arrival followed by a second one that corresponds to the shear wave arrival. In the far field, the emission pattern for the longitudinal and the shear wave presents symmetrical lobes inclined strongly off the normal (the order of 30° for shear waves to more than 60° for longitudinal waves) and there is no emission along the normal ⁹. Note that it is possible to modify the directivity of emission in the far field by having an ensemble of point sources phased in such a way that the various contributions add up at a particular location or along a particular direction. This phased array source can be implemented by sending the generation beam through several optical fibers of lengths chosen to give proper time delays ¹⁰. This method is not very flexible, so the use of separate lasers triggered at proper times has been explored ¹¹, although such a system appears too complex and too costly to be used in practice. Another scheme worth noting is the use of a ring illumination source (practically realized by focusing with a conical lens or axicon), which has the effect of concentrating energy along the axis normal to the surface and passing through the center of the ring (i.e. in other words to focus emitted ultrasound along this axis) ¹².

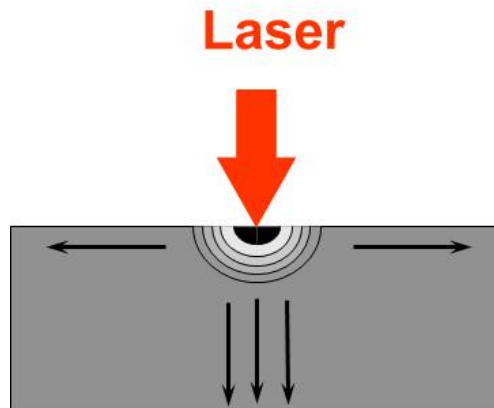


Figure 2. Thermoelastic generation

In order to have emission along the normal to the surface in the far field, which is desirable for many applications, there should be some light penetration resulting in a thermoelastic source that is buried underneath the surface. The effect of light penetration can easily be understood by considering the laser heated zone as an ensemble of slices, as shown in figure 3. As shown in the figure, each slice gives at an observation point inside the medium a displacement compression wavefront first, followed by a displacement rarefaction wavefront after reflection by the free surface and delayed by $2d/V_L$, where d is the slice depth and V_L the longitudinal velocity. These two displacements have opposite polarity but the same magnitude and rise time (equal to the laser pulse duration τ_L). The actual displacement pulse observed in the medium results from the sum from these two contributions. Therefore, when penetration is very small the displacement pulse is nearly zero, which is the case for metals at frequencies in the range

of 1 MHz to about 1 GHz (but not at higher frequencies or for very short pulses, when the typical penetration of 5 to 10 nm for metals becomes comparable to the acoustic wavelength). When penetration increases, the displacement pulse starts to increase and its shape is found to follow proportionally that of the laser pulse. With further increase of light penetration, when the penetration depth becomes about τV_L , the displacement pulse amplitude saturates and its width increases.

This qualitative explanation above can be made easily quantitative and an analytical expression can be readily obtained if the laser pulse shape can be described analytically¹³⁻¹⁵. Further to this unidimensional model, 3-D cases have been treated assuming axisymmetric¹⁶ and orthotropic media¹⁷. Light penetration has been experimentally studied in detail with colored glasses giving a wide range of penetration depths^{15,18}. Light penetration is very important in practice since it gives a piston source at the surface of the material emitting normally propagating longitudinal waves, independently of the surface curvature and of the orientation of the laser beam. This is at the basis of the inspection of polymer-matrix composites, which is one of the industrial applications of laser-ultrasonics (see figure 4).

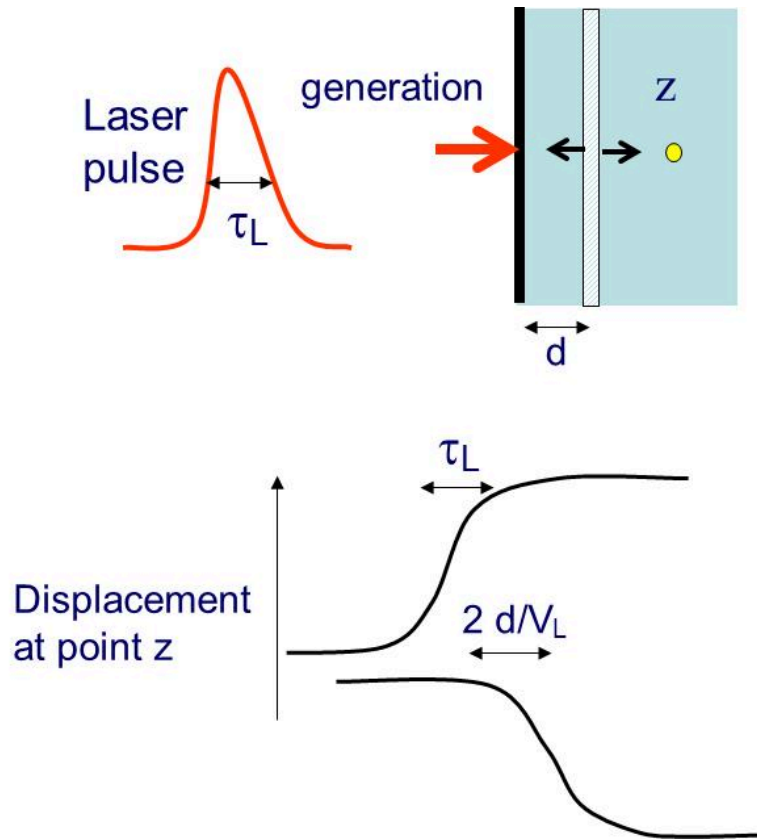


Figure 3. Thermoelastic generation with penetrating light. Upper: the figure shows schematically a laser pulse of duration τ_L and a layer at depth d heated by this laser pulse in a given medium. An observation point is shown in this medium at depth z . Lower: the figure shows schematically the two displacement signals observed at point z , one being associated to a compression and arriving directly at z and the other one being associated to a rarefaction and reaching z after reflection by the free surface. The actual displacement at z results from the sum of these two signals.

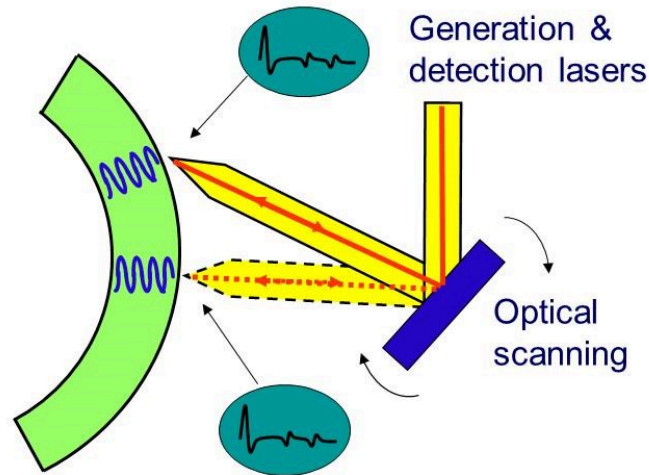


Figure 4. Effect of penetrating laser light: generation occurs perpendicularly as if a conventional piezoelectric transducer was moved over the surface.

Enhancement of generation along the normal also occurs when the absorbing material is covered by a transparent layer¹⁹. In this case, as explained above for the penetrating light source, there are also two delayed and opposite polarity displacement wavefronts that do not cancel if the layer is sufficiently thick. This occurs even if the material has practically no light penetration (metals).

Surface waves and plate waves can also be generated efficiently and in a very versatile manner. When the laser beam is focused to a small circular spot, a surface wave with a cylindrical symmetry is emitted from this spot. Its amplitude has a maximum when the laser pulse duration is about D/V_R where D is the spot diameter and V_R the Rayleigh velocity of the material²⁰. Detailed theoretical analysis has been performed and verified experimentally²¹. Good directivity is obtained by focusing the beam with a cylindrical lens to get a line source²². More complicated patterns can even be used, such as an array of lines, giving narrower band emission but having the advantage to distribute the laser energy over a broader area, so ablation and surface damage can be avoided. A chirp array has also been used in combination with a matched pattern used for detection²³, as well as a pattern obtained by using a computer-generated hologram or a spatial light modulator²⁴. A converging circular Rayleigh surface wave giving very strong displacement at the center of convergence can be readily obtained by using, in addition to the conventional spherical lens, an axicon (conical lens)²⁵. Of course, when the thickness of the sample becomes of the order of the Rayleigh wavelength or less than it, dispersion effects of plate waves should be taken into account. When a line source is used, emission can be strongly enhanced by sweeping the laser line over the surface of the sample (for example by reflecting the laser beam off a fast rotating mirror)²⁶: enhancement occurs when the sweeping velocity of the laser beam is equal to the Rayleigh velocity V_R . With a grating source, strong enhancement is observed when the grating is made to move with a velocity equal also to the Rayleigh velocity²⁶. Such a moving grating can be obtained by making two beams issued from the same generation laser to intersect at the surface of the sample, one being frequency shifted by an offset f (for example by sending it through an acousto-optic shifter). By reference to figure 5, the enhancement condition is: $\lambda/2\sin\theta = V_R/f$, where λ is the optical wavelength and θ the angle between the laser beams and the normal (note that $(f\lambda)/(2\sin\theta)$ is the grating velocity).

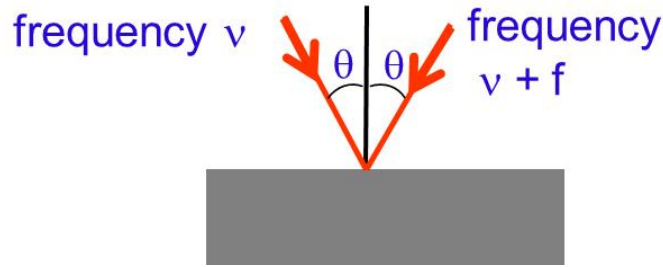


Figure 5. Rayleigh surface wave enhancement by moving line grating.

2.2 Generation by ablation or vaporization

If one increases the energy density, particularly for small light penetration (metals), one reaches the threshold where the surface starts to melt and then to get vaporized. At this point, matter is ejected from the surface and through various physical processes this vapor and the surrounding air is ionized, thus producing a plasma plume that expands away from the laser spot on the surface (sketched in Figure 6). On the opposite surface of a plate-like sample, one first observes a surface elevation spike of duration of the order of the laser pulse duration, which is associated with the recoil effect produced by the matter blown off the surface. This displacement then continues all the time the plasma applies a pressure on the surface and diminishes with plasma expansion and cooling. Therefore, depending upon the energy density, the phenomena taking place goes from solely a vaporization effect for which the ultrasonic pulse has duration of the order of the laser pulse to a strong plasma regime with a much longer duration⁴⁻⁶. A similar vaporization effect occurs also when the material is covered by a thin absorbing layer, which is blown off, leaving the substrate underneath substantially unaffected if the energy density is below some threshold. In the strong plasma regime on the other hand, a crater mark is left on the surface (as sketched in figure 6). It should also be noted that in addition of vaporization and plasma contributions, there is always some thermoelastic contribution, which is clearly or barely noticeable depending upon the regime.

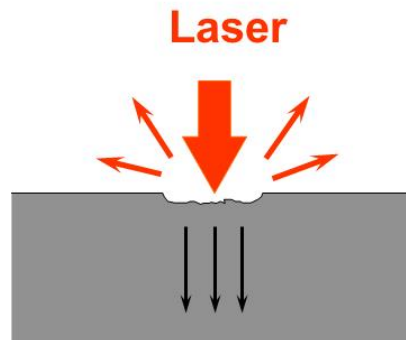


Figure 6. Generation by ablation or vaporization. In the case of strong ablation, a crater is left on the surface.

The generation by ablation has not been modeled as well as thermoelastic generation, for which precise computer codes have been written. Some modeling has however been performed^{27,28,29}. The vaporization regime or ablation in vacuum can be modeled relatively easily³⁰. An approximate description has been obtained by assuming that the effect is represented by a surface force pointing inwards with appropriate duration^{4,5}. When this surface force is combined with a thermoelastic dipole, all

the generation conditions can actually be described. This approach also allows predicting the far field patterns^{4,5} that have been experimentally observed.

3. Laser detection of ultrasound

To detect ultrasound, the surface is illuminated by a laser beam, continuous or of pulse duration sufficiently long to capture all the ultrasonic signal of interest. Scattered or reflected light is then collected by an optical receiver that could be either based on an interferometer or on a non-interferometric device. Practically useful non-interferometric schemes are based on the detection of the change of reflectivity produced by the ultrasonic strain or the knife-edge technique³¹. The detection of the change of reflectivity, which is of the order of the ultrasonic strain and small (in the 10^{-4} to 10^{-6} range) is particularly useful at high frequencies since strain increases proportionally to frequency for a given displacement. The knife-edge technique on the other hand is based on monitoring with a knife edge positioned in front of a detector or with a position sensitive detector the tilt produced by the ultrasonic surface ripple. This very simple to implement and quite sensitive technique, is however limited to polished surfaces and laboratory experimentation.

Regarding interferometric techniques, it is first useful to recall the effect of the ultrasonic surface motion on the scattered or reflected light. A surface displacement $\delta(t)$ produces a shift $4\pi\delta(t)/\lambda$ on the phase $2\pi\nu t$ of the backscattered or reflected light field, where ν and λ are the optical frequency and wavelength, respectively. This phase can be readily rewritten to show that the instantaneous frequency is changed to $\nu(1 - 2V(t)/c)$, which expresses the well known Doppler effect and where $V(t)$ is the ultrasonic surface velocity ($V=d\delta(t)/dt$). Further, assuming surface motion at a frequency f , simple trigonometric manipulation shows that the backscattered or reflected field includes 3 terms: a central carrier at the laser frequency ν plus two optical sidebands at frequencies $\nu+f$ and $\nu-f$. The ratio of the field amplitudes between the sidebands and the central carrier is $2\pi U/\lambda$, where U is the ultrasonic surface displacement amplitude. When the surface motion is not a single frequency, the sidebands are broadened into two symmetric lobes on both sides of the carrier optical frequency ν . These three descriptions of the effect of the surface motion are equivalent and any one could be used to interpret any interferometric detection scheme.

Interferometric detection is based on the conversion by the interferometer of the phase or frequency modulation produced by the surface motion into an intensity modulation, which is detected by the optical detector, as schematically represented in figure 7^{31,32}. Regarding sensitivity of interferometric detection, it should be noted that there is a fundamental limitation associated with the nature of light as an ensemble of discrete particles. The minimum displacement that can be detected is a function of the number of collected photons and is given by the following formula: $\delta_{lim} = (\lambda/4\pi) (B h\nu/ 2\eta P_0)^{1/2}$, where h is the Plank's constant, η the quantum efficiency of the detector, B the electronic bandwidth and P_0 the collected power³³. This formula assumes optimum conditions: the optical field scattered by the surface coherently and uniformly interferes with a much more intense reference wave (without phase or frequency modulation or optical sidebands) directly derived from the detection laser, i.e. there should be no speckle effect and perfectly matched signal and reference wavefronts. This formula also assumes a quadrature condition between signal and reference. For example, for $\lambda= 1.06 \mu\text{m}$ and $\eta= 0.9$, the ultimate sensitivity is $3 \times 10^{-8} \text{ nm (W/Hz)}^{1/2}$ or 0.003 nm for 1 mW received and 10 MHz bandwidth. It should be noted that this sensitivity is the ultimate that can be obtained with the classical light fields produced by all existing lasers, but it can be improved in principle by using squeezed states or other non-classical states of light³⁴. When working with a speckled signal beam, the sensitivity is reduced well below the ultimate

limit unless the interferometer also acts as a signal-to-reference wavefront adapter or one speckle is collected.

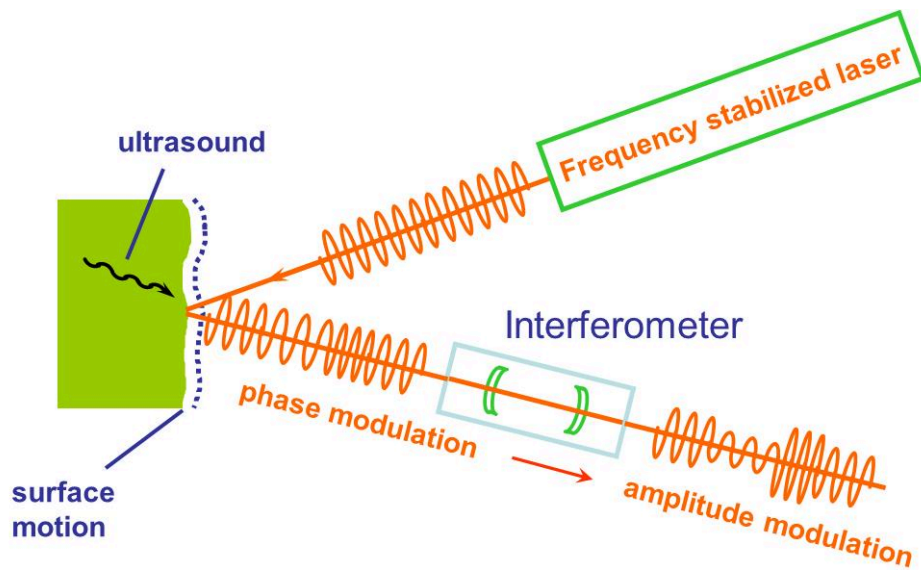


Figure 7. Principle of optical detection of ultrasound with an interferometer: the interferometer converts the phase or frequency modulation produced by the surface motion in an intensity modulation.

A simple Michelson interferometer, sketched in figure 8, has been used for many years for laboratory experimentation. Its drawback for use in industry (except in conditions where the surfaces are polished or smooth, such as in the microelectronic industry) is its sensitivity to optical speckle. Any optical device has some capacity to collect scattered light, called its etendue or throughput, which is defined as the product of the surface of the illuminated spot by the solid angle of the input aperture seen from the surface. In the case of the simple Michelson interferometer of figure 8, this parameter is small and of the order of the square of the optical wavelength (about $10^{-6} \text{ mm}^2 \cdot \text{sr}$), which in practice requires to focus the beam onto the surface to collect essentially one speckle³¹. One will note that the surface is actually in this scheme part of the interferometer as one of its mirrors.

The limitation of one speckle detection can be circumvented by using a matrix of detectors that detects several speckles and by combining the various signals from the detectors. A reported system has several channels each being based on a quadrature Michelson interferometer³¹. Each channel provides either the square of the ultrasonic displacement or the displacement itself, depending upon the number of detectors used per channel and signal processing^{35,36}.

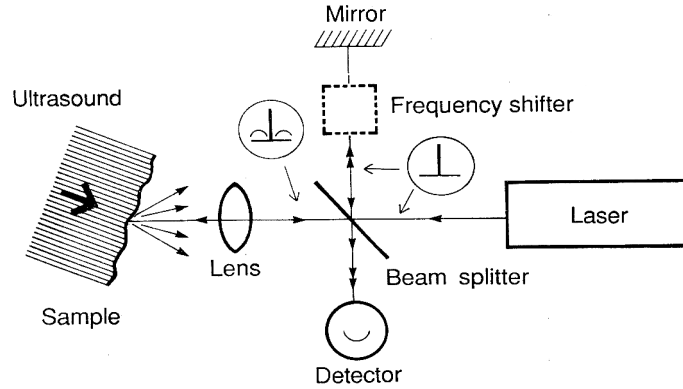


Figure 8. Michelson interferometer: the inserts indicate schematically the optical spectra along the reference and beam paths.

Still, a more practical scheme is to use the Michelson interferometer as a light filter working as a frequency analyzer of the scattered light ³⁷. Such a filtering action is obtained by giving very different pathlengths to the two arms of the interferometer. The two interfering waves in the interferometer are then given a time-delay (time-delay interferometry), which should be of the order of half the ultrasonic period for optimum sensitivity. For the frequency range of 1 to 20 MHz, this results into a very bulky system, particularly if immersion in a liquid bath is added to increase etendue. A much more practical implementation of time-delay interferometry and demodulation by an optical filter is based on the use of multiple beam interference in the confocal Fabry-Perot interferometer.

3.1 Confocal Fabry-Perot interferometer

This is a simple optical resonator made of two concave identical mirrors separated by a distance equal to their radius of curvature L_R ³⁸. As shown in figure 9, any incident ray gives 4 rays, two on the transmission side and two in reflection. In excellent approximation each ray retraces its path after multiple reflections in the resonator and the multiple beam interference phenomenon occurs on the 4 output ports. Since this takes place independently of the direction and height of the incident ray, the system has a large etendue. For example, a meter long cavity with mirrors with 85% reflectivity provides an etendue exceeding that of a collecting optical fiber with core diameter of 1 mm and numerical aperture of 0.35 (etendue equal to 0.4 mm².sr).

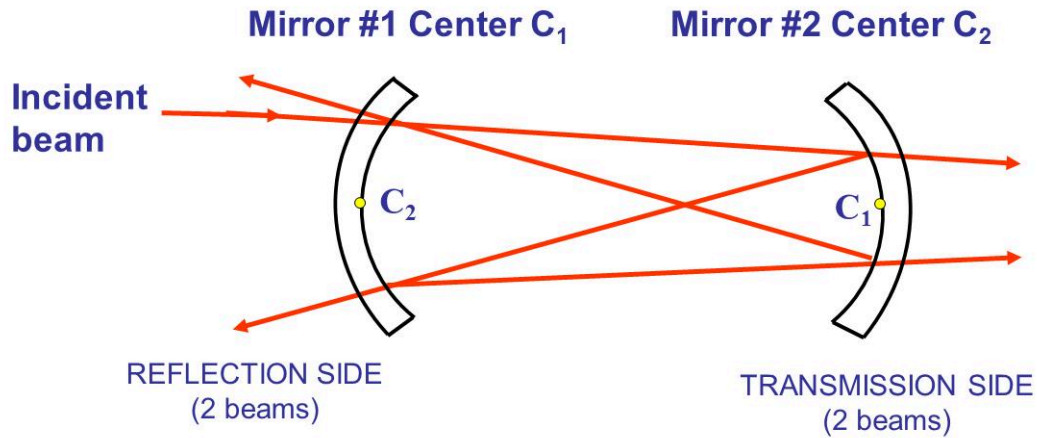


Figure 9. Schematic of the confocal Fabry-Perot interferometer.

This system is a resonator that has resonance peaks of width $\Delta\nu_{FP}$, which decreases with increased mirror reflectivity R ($\Delta\nu_{FP} = (c/4L_R)/F$, where c is the speed of light and F the finesse, $F = \pi R/(1-R^2)$). As shown in figure 10, demodulation is realized by locating the detection laser frequency on the slope of one peak³¹. Note that this interpretation, which shows that the system responds as a velocimeter (the frequency modulation of the scattered light is proportional to the surface velocity, as mentioned above) is valid only at low frequencies (frequencies much below $\Delta\nu_{FP}$). When the frequency increases to about $\Delta\nu_{FP}$, the response levels off and has to be calculated^{39,40}. Figure 11 shows the calculated responsivities and their experimental verification for two confocal Fabry-Perot configurations. In one configuration, the system is used in transmission (detector on the transmission side) and in the other one it is used in reflection (detector on the reflection side, also called sidebands stripping scheme)⁴¹. The reflection scheme has nearly flat frequency response above $\Delta\nu_{FP}$ (except for the periodic drops every $c/4L_R$) and will be used preferably for detection in this high frequency range. It should be noted that the responsivity is practically zero at very low frequencies, which means that this system is intrinsically insensitive to vibrations, a key advantage for use in industrial environments.

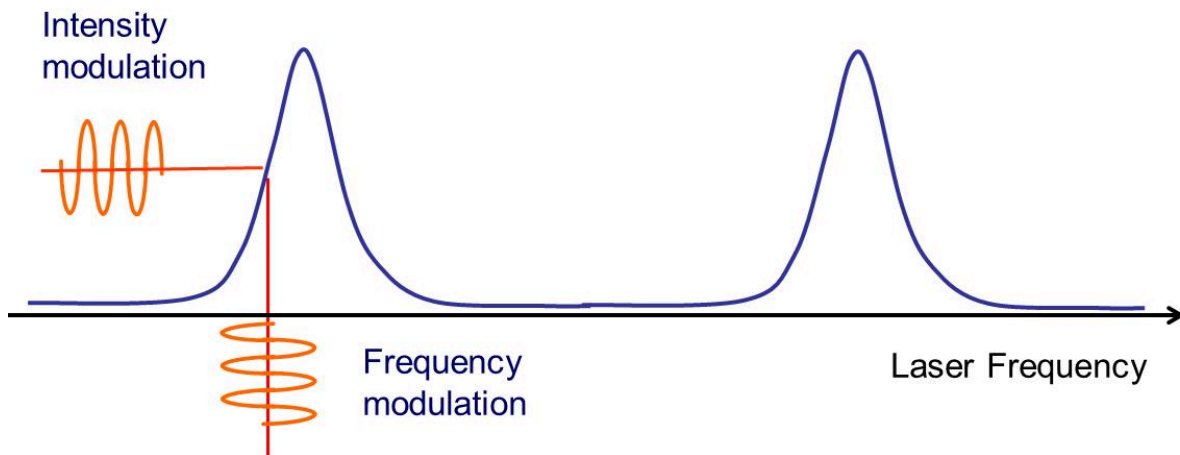


Figure 10. Principle of demodulation with a confocal Fabry-Perot

Regarding sensitivity, the minimum detectable displacement is about $4 \delta_{\text{lim}}$ at maximum response for the transmission and reflection configurations. When high sensitivity is only required at high frequencies, the back mirror could be made totally reflecting. This leads to improved sensitivity by about a factor two. This can be explained by the fact that the four output beams exiting a confocal cavity, two on the transmission side and another two on the reflection side, giving four independent output ports with multiple interference on each port, are now reduced to two, contributing to an increase of the intensity of interfering terms and consequently of sensitivity. A further improvement by $\sqrt{2}$ can be obtained with a configuration with only a single output port on the reflection side. This can be realized with a totally reflecting back mirror and a front mirror that is totally reflecting over half of its surface, as in the original confocal Fabry-Perot design^{33,38}. It should also be noted that the transmission scheme could operate with unpolarized light whereas the use in reflection requires polarizing optics for optimum operation. Therefore often in practice, especially if a large core multimode fiber is used to transmit light to the Fabry-Perot, the transmission configuration gains a sensitivity factor of about $\sqrt{2}$ with respect to the others. If the range of frequencies of interest is between 1 and 15 MHz, which is often the case in industrial nondestructive testing, this configuration will be the one usually selected with a proper choice of mirror reflectivity R and cavity length L_R to give adequate etendue and frequency response.

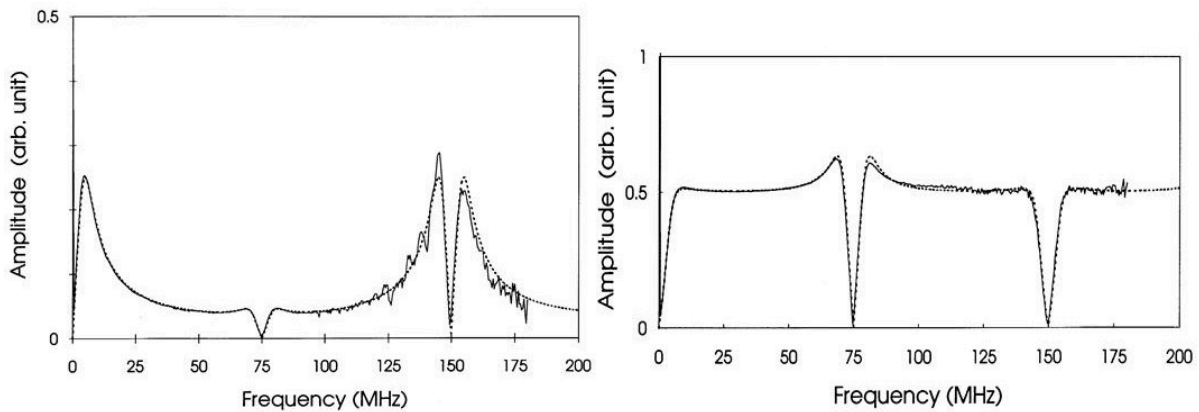


Figure 11. Frequency response of a confocal Fabry-Perot 1 m long used in transmission (left) and in reflection (right) ; full line: experimental data, dash line: calculated data.

The main weakness of the Fabry-Perot demodulators is their lack of sensitivity at low ultrasonic frequencies (below 2 MHz), which is circumvented by the devices based on two-wave mixing in photorefractive materials described below. Regarding the reduction of the effect of laser noise, a differential scheme which eliminates or at least minimizes laser intensity noise has been reported⁴². More recently another one, more powerful which eliminates in addition phase noise has been described⁴³.

3.2 Photorefractive two-wave mixing interferometer

In the two-wave mixing approach, wavefront adaptation is performed actively, by opposition to the confocal Fabry-Perot in which adaptation is performed by passive or linear optical components; the technique used is also known as real-time holography. This active wavefront adaptation eliminates the need of an external stabilization device against thermal drift or ambient vibrations, as required for the confocal Fabry-Perot. The basic setup of the two-wave mixing interferometer is sketched in figure 12. A

signal beam which acquires phase shift and speckle after reflection on a surface in ultrasonic motion, is mixed in a photorefractive crystal with a pump plane wave to produce a speckle adapted reference wave that propagates in the same direction as the transmitted signal wave and interferes with it. The quadrature condition is provided by passive optical components after the crystal ^{44,45}.

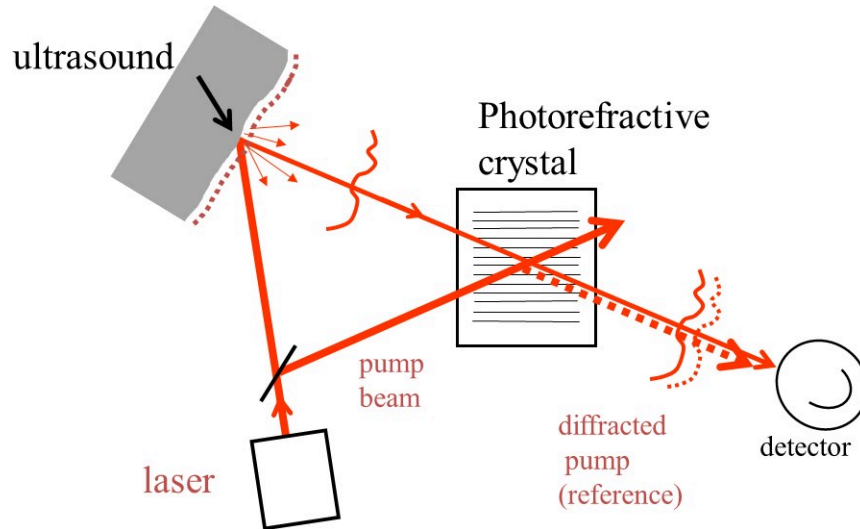


Figure 12. Demodulation with a two-wave mixing photorefractive interferometer

The etendue, determined by the size of the crystal and the angle between the signal and pump beams, is easily made larger than the etendue of the fiber mentioned above. The response of such a device is flat from a low cut-off frequency f_c , which depends on crystal properties and pump intensity, up to the detector cut-off frequency. There are no periodic sensitivity drops like in the confocal Fabry-Perot. With an InP crystal with proper iron doping, operating at $1.06 \mu\text{m}$ and with the application of an electric field, the sensitivity is about the same as the maximum sensitivity of the confocal Fabry-Perot used in transmission, i.e. the detection limit is about $4 \delta_{\text{lim}}$ ⁴⁶. Better sensitivity has been demonstrated with a CdTe crystal with Vanadium doping ⁴⁷, but CdTe photorefractive crystals need further development before becoming a reliable source for such a device. At $1.06 \mu\text{m}$, GaAs crystals are also used without an electric field giving a sensitivity reduced by about 2.5 compared to the maximum sensitivity of the confocal Fabry-Perot ^{45,48}.

One important advantage of the photorefractive demodulator with respect to the confocal Fabry-Perot is its better sensitivity at low ultrasonic frequencies (below 1 MHz), thus allowing probing more easily materials with strong ultrasonic attenuation (materials with coarse microstructure, porous or mushy materials...). The system has also the advantage to be easily combined with a differential or balanced scheme (two detectors giving responses to phase modulation of opposite sign), so the noise coming from the laser intensity fluctuations can be eliminated to a large extent ⁴⁹. Further, by making the pathlengths from the laser to the crystal along the signal and the pump beams to be sensibly equal, the effect of laser phase noise is eliminated.

Its weakness, in spite of the use of semiconductor photorefractive crystals with high photoconductivity (GaAs, InP, CdTe), is its rather slow response time, i.e. the time needed for the photorefractive grating to be built up or to be erased. This affects the ability of the system to adapt to motions of the probed object that cause a change of the speckle pattern of the scattered light or a change of its frequency by the

Doppler effect. This time τ_c is related to the low cut-off frequency f_c by the relation $\tau_c = 1/(2\pi f_c)$. The response time also scales essentially as $1/\text{pumping intensity}$. Responses times as short as 400 ns are obtained at 1.06 μm with an intensity of about 3 kW/cm^2 in a GaAs crystal without an applied electric field. The application of an electric field, which increases sensitivity, has however the drawback to lengthen the response time. With an InP:Fe crystal under a field of 4.9 kV/cm and a power density of about 100 W/cm^2 , a time constant of about 2 μs is obtained ⁴⁶. These values are longer than those typically obtained with a confocal Fabry-Perot, which can be estimated as $(4 L_R/c)F$. For a one-meter long Fabry-Perot with a finesse of 10 or a 50 cm long with a finesse of 20, this gives $\tau_c \approx 130$ ns. This means that this system cannot be used as easily as the confocal Fabry-Perot on moving objects. Motion of the object along the line-of-sight causes a Doppler shift (Doppler shift $\Delta\nu = 2V/\lambda$, where V is the projected velocity along the line-of-sight) which diminishes strongly the responsivity. For example a GaAs crystal pumped with 350 mW has a response time of about 35 μs and its responsivity drops more than 50% for a Doppler shift of 10kHz corresponding to $V=0.5$ cm/s). To be unaffected by a velocity of 1m/s would require a response time τ_c much less than 1 μs .

It should be noted that the photorefractive system is much more tolerant to motions transverse to the line-of-sight that cause only a change of the speckle pattern without a change of frequency. Although the effect of sensitivity reduction by the object motion along the line-of-sight or transverse has not been thoroughly investigated, it can be understood that a displacement of $\lambda/2$ or less during the time τ_c causes grating washout ⁴⁶, whereas the displacement should be much larger (the size of a speckle) to produce speckle decorrelation and a corresponding reduction of sensitivity if there is only transverse displacement.

To compensate for the Doppler shift, the frequency of one of the interfering beams can be changed (for example by sending the beam through an acoustooptic shifter) in such a way that the photorefractive grating becomes stationary in spite of the object motion. An automatic system that performs this compensation has been demonstrated and is based on the tracking of the error signal that appears at the output of the balanced receiver or differential amplifier after the crystal ⁵⁰.

3.3 Imaging and multiplexing with a photorefractive two-wave mixing interferometer

Any optical receiver that has a sizable etendue can demodulate over several spots in parallel or over an image. Although this can be demonstrated with the confocal Fabry-Perot (using the Connes type to avoid spurious superposition of images), this is more easily implemented with a photorefractive two-wave mixing interferometer. In the multiplex scheme, as shown in figure 13, several spots are projected onto the surface of the tested objects according to an arrangement that fits the application (line, grid array, circle...). Scattered light from these spots is then projected onto the photorefractive crystal, either at distinct locations or at the same location from different directions and is finally received by separate detector elements ^{51,52}. In this last case, it can be shown that there is essentially no cross talk between the various channels when the pump intensity is much larger than the intensity of any signal beam. Such a configuration can obviously be used to increase the speed or throughput of an inspection task by the number of spots but can also be applied for realizing a focusing detector. For example, if the spots are distributed along a line, the system has a peaked response for a surface wave incident perpendicularly to the line. If the spots are on the other hand located on a circle, the system detects essentially a surface wave originating from the center of the circle.

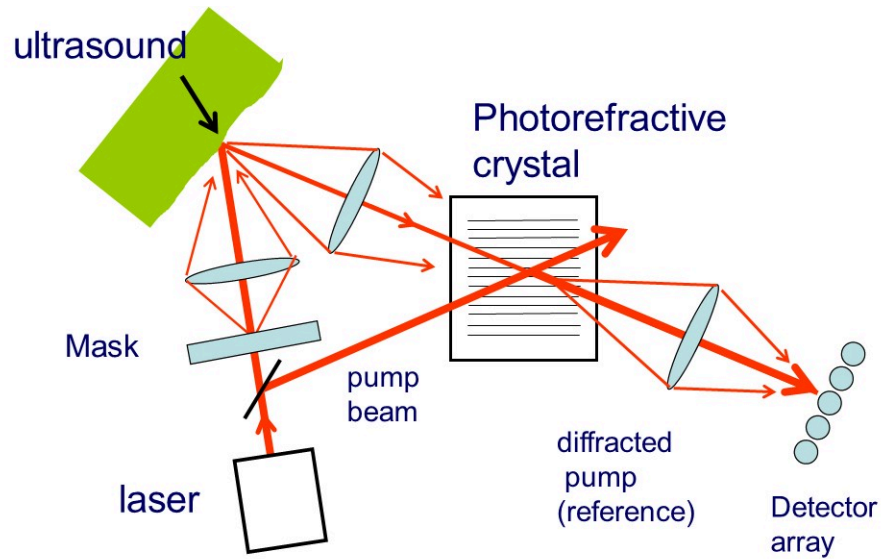


Fig. 13. Sketch of an optical multiplexing scheme associated with a photorefractive demodulator. The mask could be replaced by other optical elements such as an holographic grating or a fiber bundle array to project a light spot distribution onto the surface of the object.

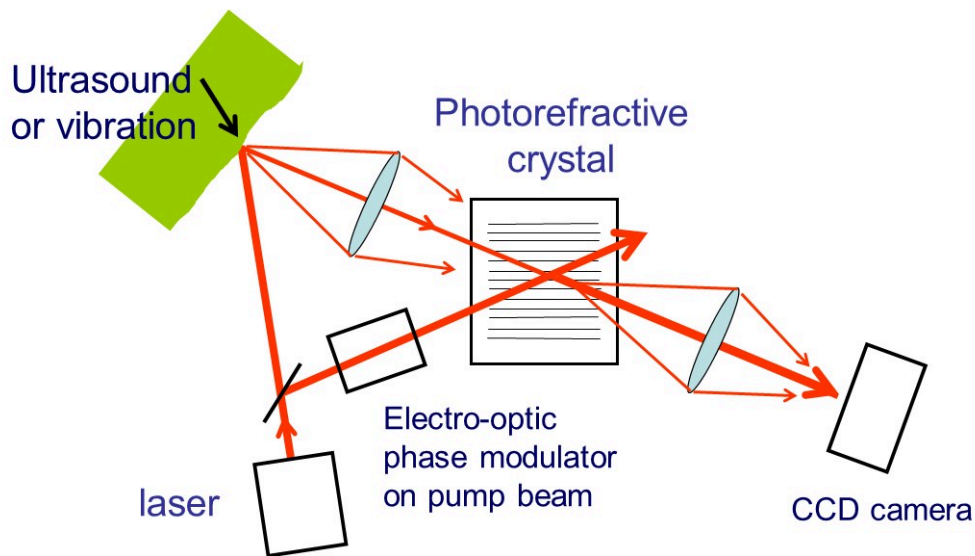


Figure 14. Sketch of full field imaging of vibration or ultrasonic motion with a photorefractive demodulator.

Full field imaging of vibration or ultrasonic motion at the surface of an object can be obtained with the setup sketched in figure 14. The pump beam is strongly phase modulated at a frequency close to that of the surface disturbance to be detected (the difference of frequencies should be less than the photorefractive crystal low cut-off frequency f_c). This modulated pump has essentially the effect to produce inside the crystal a photorefractive grating that is nearly stationary and diffracts a beam that

interferes with the transmitted signal beam. Then, at each point across the crystal or across an image of the surface, a signal representative of the surface displacement at this point is obtained and could be seen on a CCD camera^{53,54}.

3.4 Other interferometric detection schemes

Two interferometric detection schemes are worth to be mentioned due to their low implementation cost in spite of many practical limitations. A first one is based on a Sagnac interferometer and is sketched in figure 15. The interferometer uses single mode fiber preserving polarization and include two fiber paths from the source to the probe surface, a long path and a short path linked with fiber couplers and making a loop. The signal comes from the interference of optical beams having travelled along the loop in opposite directions. The phase shift between these beams is therefore produced by the surface motion at two different times, the time for going from the source to the surface along the short path and the time for going along the long path. Since these interfering beams travel along the same path the interferometer is by itself self-referencing. Further analysis shows that the interferometer is sensitive to the surface velocity like the time-delay Michelson mentioned above and that the maximum signal is obtained when the time delay between the long and short path is half an ultrasonic period. As it is usually the case, the interfering beams should be in quadrature, which is realized in practice by a phase modulator⁵⁵ or an electro-optic modulator driven by a ramp signal⁵⁶ or a quarter wave plate (or its equivalent realized with a fiber polarization controller) in front of the detector (assuming well preserved polarization along the two fiber paths)⁵⁷.

The drawback of the Sagnac approach is the need to use single mode fiber to preserve spatial coherence within the interferometer and as a consequence this system has a very low etendue, about the square of the wavelength like the simple Michelson interferometer mentioned above and shown in figure 8, i.e. typically 5 orders of magnitude compared to the etendue of a 1mm core multimode fiber that is well accepted by the confocal Fabry-Perot or photorefractive interferometers. This means in turn single speckle collection and need to focus onto the surface to near-diffraction limited spot.

The other one which very cost effective (called CHOT for Cheap Optical Transducer or d-CHOT, d standing for detection) uses a periodic mask (grating) which is deposited onto the surface^{58,59}. This grating is illuminated by a laser and the zero order diffracted beam is only detected. The quadrature condition between the interfering beams from the masked and unmasked areas is obtained by making the thickness of the masking area to be 1/8 optical wavelength. This optical transducer is particularly useful for detecting surface waves that have been generated by illuminating a similar mask (called g-CHOT) with a pulsed laser. Optimum sensitivity is obtained when the period of the mask corresponds to the acoustic wavelength. The main limitation of this very cost effective approach is the need to attach the transducers (detection or detection plus generation) to the surface of the part.

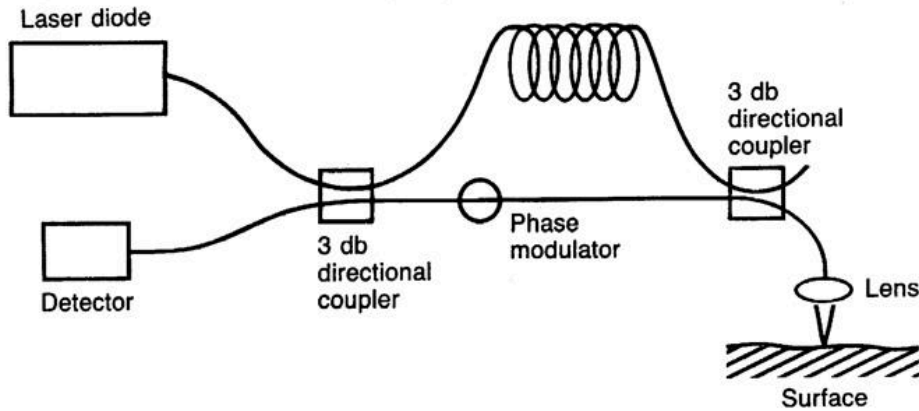


Figure 15: sketch of a Sagnac fiber interferometer for ultrasound detection

3.4 Detection laser

One key element of the detection scheme is the detection laser. It should be high power, since sensitivity increases with power, and should not contribute to any noise in addition to the fundamental photon or shot noise. High power is particularly needed when the surface is absorbing and detection is at a large distance giving a small collection solid angle. The pulse duration should be sufficiently long to capture all the signal of interest, which means for many applications a duration between 10 and 100 μ s. Nd-YAG technology at 1.06 μ m, which is known to provide high amplification gain, is particularly suited for realizing such a laser by amplifying a small and very stable Nd-YAG laser oscillator⁶⁰. Suitable single frequency oscillators are commercially available with power from 100 mW to several watts and are based on a small monolithic cavity pumped by a laser diode⁶¹. Depending upon the repetition rate, the amplifier could be flashlamp pumped (up to 100 Hz) or diode pumped (above 100 Hz)⁶². Faraday isolators are typically used after the small laser oscillator and between amplification stages to prevent feedback and spurious oscillations in such a high gain system. Peak powers of several hundred watts and more are typically obtained with pulse duration of the order of 50 μ s.

The effect of the additional noise in laser amplifiers that originates from the Amplified Spontaneous Emission (ASE) has been studied for two possible configurations: the amplifier is located ahead of the probed object (pre-amplification scheme) or after it (post-amplification scheme). Pre-amplification is generally preferable because ASE is attenuated by surface absorption and collection losses in the same proportion as the signal beam, making this additional noise negligible in comparison to the shot noise⁶³.

Alternatively, since such a master oscillator-pulsed amplifier system is complex and costly, a pulsed oscillator without seeding by a low power oscillator could be considered, as it was the case for early work in laser-ultrasonics³⁷. In this case, detection should be performed over a region of the pulse where the strong relaxation oscillations present at the beginning of the pulse have been sufficiently damped. A system with a plateau with power of more than ten watts, lasting about 100 μ s with weak residual oscillations has been demonstrated⁶⁴. This system provided single transverse and longitudinal mode, either with flashlamp or diode pumping and was best used with a photorefractive demodulator with balanced receiver to eliminate any residual oscillations from the output signal.

In the case in which the Sagnac interferometric approach is used, the source should have a short coherence length to avoid additional and undesirable interferometric contributions. This is realized with a super luminescent diode, which in practice cannot have the power that could be obtained with an amplified single frequency source.

4. Digital Signal Processing

Laser-ultrasonics, like any other ultrasonic technique could benefit advantageously of digital signal processing to increase sensitivity. Operations such as averaging, adaptive filtering could be used as well as more advanced methods such as split-spectrum processing or wavelet denoising.

Regarding imaging, a numerical imaging approach such as the one based on the Synthetic Aperture Focusing Technique (SAFT) can be combined with laser-ultrasonics to obtain high quality images^{65,66,67}. The principle of SAFT is explained by reference to figure 16 as follows. An array of signals is obtained by generating and detecting ultrasound over a grid of points. A point P in the volume of the object is interrogated by summing in a computer all the signals with a proper delay. The delay applied corresponds to the propagation time between the point P and the generation/detection point from the grid at the origin of the signal. If, after summation a result above a certain noise threshold is obtained, this is indicative of a flaw at the point P. Otherwise, there is no flaw at P. Since such processing performed in the time domain can be very computation intensive and fairly long, methods that operate in Fourier space and make use of Fast Fourier Transform algorithms have been developed. These methods, significantly different from the conventional time SAFT, although sometimes called F-SAFT, are based on a plane wave decomposition of the acoustic field for each frequency combined with a back-propagation algorithm^{68,69,70}. It should also be noted that SAFT processing could be applied to laser generated surface and plate waves⁷¹.

More recently, following developments done with conventional phase-array transducers, the technique of Full Matrix Capture combined with the Total Focusing Method was explored by laser-ultrasonics⁷². This approach is expected to provide some improvement over SAFT but since data is acquired over all combinations of the emission and detection points it may take too much time to be used in practice.

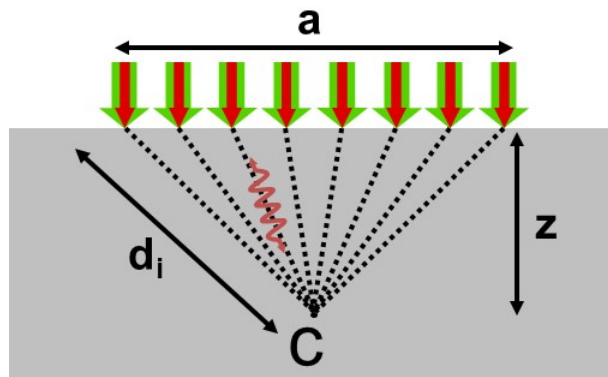


Figure 16. Principle of laser-ultrasonic SAFT processing

5. Industrial applications

Laser-ultrasonics has been the object of continuous efforts by the scientific and research community to better understand the phenomena taken place during generation and detection of ultrasound and to devise ways to make it usable in an industrial environment. These ways have aimed to push sensitivity, increase bandwidth and insure robustness and reliable operation in spite of ambient disturbances (such as vibrations). However, implementation of the technique is complex, particularly in comparison with conventional piezoelectric-based ultrasonics and also costly and these factors have slowed its industrial use. Nevertheless, there have been many efforts to explore industrial applications, first in a laboratory environment, often in an industrial setting and we have seen it transitioned from year 2000 to the industrial floor for a few applications, which are described below.

As with piezoelectric-based ultrasonics, laser-ultrasonics can be used to measure thickness (after calibration for wave velocity), to detect flaws (such as cracks, pores, disbonds ...) and to characterize materials due to the sensitivity of ultrasound propagation to material microstructure. The applications that have been explored and those that have also been implemented in industry have relied on the distinguishing features of laser-ultrasonics in comparison to conventional ultrasonics, such as non-contact (testing hot products or in vacuum), complex shapes, very broad bandwidth, efficiency for surface waves generation and detection...

5.1 Thickness measurement

5.1.1 On-line wall thickness gauging of seamless tubes

The development of this application follows from collaboration between NRC and the Timken Company, which received the support of the US Department of Energy for the implantation on a Timken production line of a laser-ultrasonic wall thickness gauge. This gauge has measured reliably since its deployment millions of tubes⁷³. NRC had demonstrated the feasibility of such an application many years before on a seamless tube production line of Algoma Steel. This was also followed by similar demonstrations elsewhere⁷⁴.

The use of laser-ultrasonics in this case follows from the need of a sensor for measuring at elevated temperature right on the production line the wall thickness and eccentricity. These tubes are fabricated by hot piercing and are used in particular to make hollow round parts with added value, such as pressure cylinders, races of ball bearings... The fabrication process, consisting essentially of forcing a mandrel through a hot billet in rotation, results in relatively large thickness variations and eccentricity, which are undesirable since these variations lead to added fabrication costs for the final products (e.g. more machining time, increased tool wear). Therefore better control of the fabrication of the tubes was needed and has been made possible by the laser-ultrasonic thickness gauge installed on-line and providing in real time information on tube characteristics. This system allows in particular obtaining very quickly and reliably better mill setups, thus reducing out-of-tolerance products (less scrap and rework) and troubleshooting time. It has resulted in significant productivity increase. The technique allows in particular to measure thickness and eccentricity at the initial piercing stage when the piercing mandrel is within the tube, which is not possible with the competing technique of gamma-ray tomography.

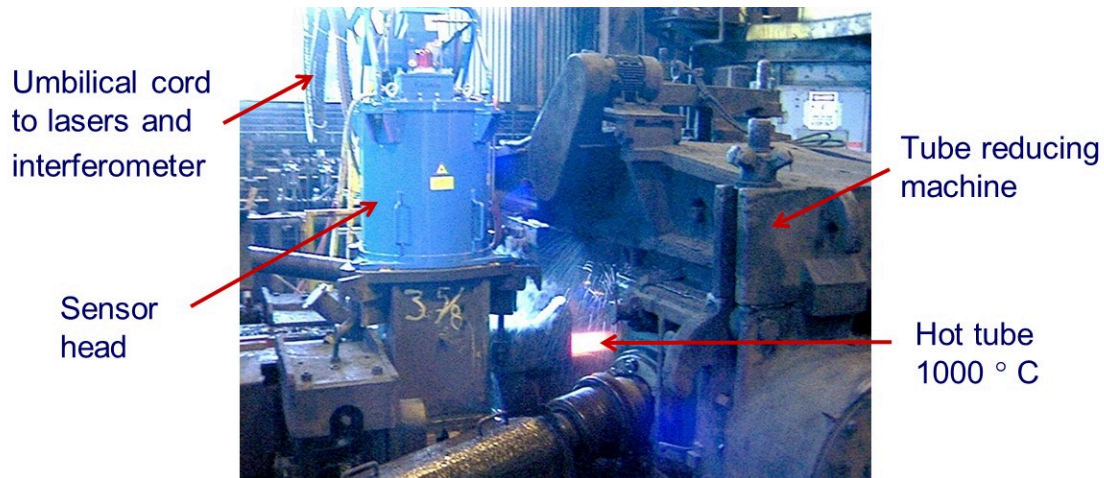


Figure 17. View of the inspection head measuring on-line a tube being processed.

Since the system has to operate in a severe industrial environment, it was made of essentially two units, an environment controlled cabin and a measuring head on top of the line linked by an umbilical cord containing optical fibers for transmission of the generation and detection laser beams and for bringing the scattered light to the interferometer. The cabin houses the lasers, the confocal Fabry-Perot interferometer, control electronics, processing and display data computers. This system also includes a fiber-coupled pyrometer to measure tube temperature and a fiber-coupled coordinate measuring system to determine the measuring locations on the passing tube in rotation and to provide full thickness mapping. A picture of the measuring head on top of the line and above a passing tube is shown in figure 17. Note that the implemented system provides eye-safe operation all the time, convenient and fast removal of the measuring head for line service or modification and adequate laser servicing (e.g. periodic flashlamp change) by the location of the lasers in a dust free clean environment. It was also found that the system could provide more than thickness information such as a measurement of the austenitic grain size by proper analysis of ultrasonic attenuation⁷⁵. Although the system at Timken has been removed from operation after measuring millions of tubes, this application has been commercialized by Tecnar Automation Inc. with several tens installations throughout the world⁷⁶.

5.1.2 Thickness determination of microelectronic thin layers

This industrial application follows from developments performed at Brown University on the generation and detection of very high frequency ultrasound with very short pulse lasers (typically femtosecond Ti:Sapphire lasers with pulse duration of about 100 fs)^{77,78}. As shown in figure 18, the short pulse laser is directed onto the tested sample, where it generates normally propagating longitudinal waves. We have seen above that such a generation is efficient because the laser pulse is very short, even if light penetration is very small, such as in metals (5 to 10 nm). For such a penetration, the propagation delay though the heated layer is even larger than the pulse duration. Therefore, in practice to resolve very thin layers that are not strongly absorbing, a thin metallic layer has to be added as a transducer layer to insure a sufficiently short pulse. This limitation is not important in practice since the technique is applied essentially to opaque thin films, transparent films being well measured by ellipsometry. The stress pulse is detected by monitoring the change of reflectivity using a stroboscopic technique: as shown in figure 18, part of the laser pulse is sent to a delay line and is used to probe the reflectivity change after a given

delay. By varying the length of the delay line, the whole ultrasonic signal coming from propagation through the sample, usually a stack of thin layers, can be retrieved. Using suitable modeling of the propagation through a multi-layer system, the thicknesses of all the layers of the stack can be determined⁷⁹. This technique has been commercialized by Rudolph Technologies Inc.⁸⁰.

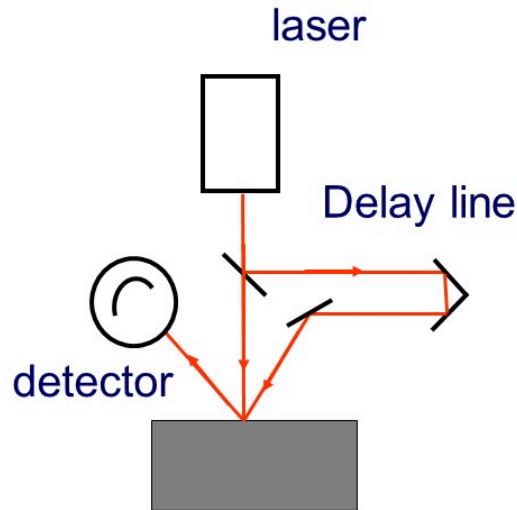


Figure 18 : Sketch of a pump-probe setup based on the change of reflectivity for detection.

5.1.3 Thickness determination and elastic properties determination of microelectronic thin layers

This industrial application follows from developments performed essentially at the Massachusetts Institute of Technology and is based on the generation of ultrasonic surface waves at the surface of the coated material^{81,82}. As shown in figure 19, two laser beams (the pump beams) interfere on the surface and produce a light grating that in turn, by thermoelastic effect, produces a surface wave with a well-defined wavelength. Actually, counter-propagating waves are produced, thus giving a standing surface wave. The time variation of this wave is then monitored by using a probe beam and detecting the beam diffracted by the surface ripple. By varying the angle between the pump beams, the wavelength or k-vector of the surface wave can be changed and its dispersion curve can be measured. Then using suitable modeling, the thickness of the layer and its elastic properties can be determined. This technique has found applications for characterizing films deposited on silicon wafers, such as the thickness measurement of copper interconnections and the determination of the mechanical properties of low permittivity films. It has been commercially developed by Philips AMS, now part of Semilab Inc.⁸³.

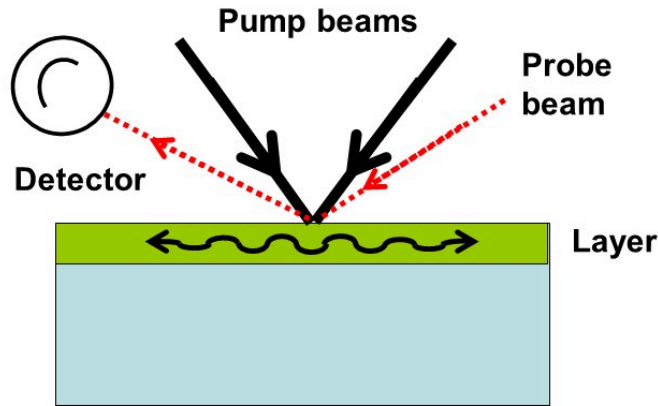


Figure 19: Sketch of a pump-probe setup based on the transient grating approach.

5.1.4 Thickness determination of other coatings

Thickness of coatings can be determined from the measurement of the reverberation time of the multiple echoes if a sufficient short ultrasonic pulse can be generated or from the corresponding reverberation frequency. Alternatively, a method based on the generation of Rayleigh waves, somehow similar to the one outlined above in 5.1.3, can be used. From a model of wave dispersion and a fit to the experimental data, owing to the very broadband that can be obtained at generation and detection, thickness can be often determined. Figure 20 show a result obtained on a thermal sprayed hard coating. In addition to thickness, the density and the elastic moduli of the coating were obtained in this case ⁸⁴.

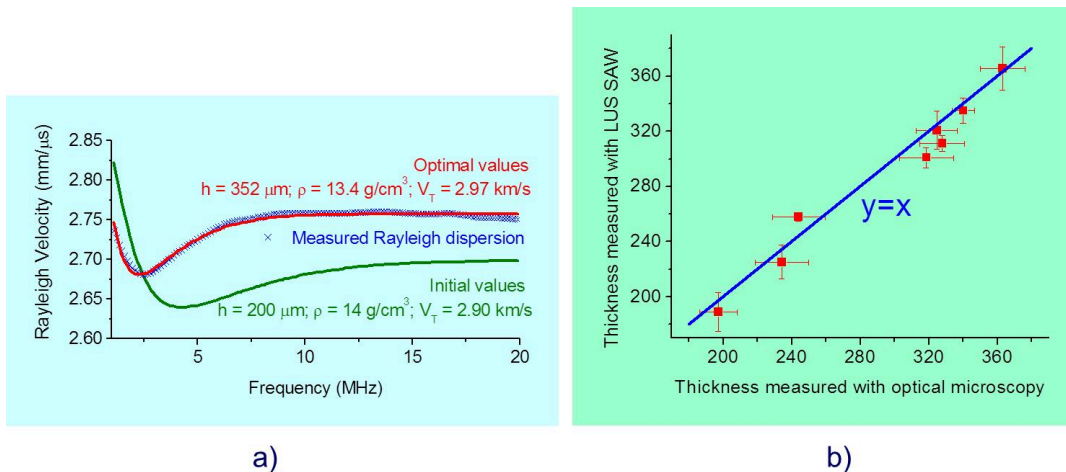


Figure 20: Thickness measurement, density and elastic moduli determination by laser ultrasonics of a thermal spray WC-Co coating; a): illustration of the fitting to the dispersion curve b): comparison of the thickness measured by laser ultrasonics with actual thickness.

5.2 Flaw detection

5.2.1 Inspection of aircraft structures made of polymer-matrix composites

The development of this application has been actively pursued for many years by NRC, UltraOptec, Inc. a licensee of NRC and General Dynamics of Forth Worth, Texas (now Lockheed Martin Aeronautics Company) ^{85,86,87}. Lockheed-Martin has at one point continued independently its own development, which has led to systems that are now routinely used for testing composite parts of the F-22 and F35 fighters manufactured by the company ^{88,89}. Laser-ultrasonics is particularly interesting for inspecting complex parts and for such parts has advantages regarding ease of operation (no additional tooling, no previous detailed knowledge of the part shape, no part precise orientation) and inspection throughput.

This application is first based on the generation of a longitudinal wave normal to the surface independently of the laser beam incident direction, as shown in figure 4. As explained above, this characteristic is based on the penetration of laser light below the surface for efficient generation and the use of a sufficiently large spot size for minimum ultrasonic beam spreading (5mm typical). For adequate absorption and penetration in these materials, a TEA CO₂ laser operating at 10.6 μm was found quite appropriate and is used in all systems built and presently in use. Penetration is about 20 μm in epoxy and of the same order of magnitude in many paints or peel-ply. Since the system should inspect large areas, a standoff distance of more than one meter is required. This requirement coupled with a scattering surface (shiny surfaces cause some difficulty, see below), which could be also highly absorbing, makes the use of a high power detection laser mandatory. In all the systems developed and presently used, this detection laser is based on Nd-YAG technology and has been described above. A confocal Fabry-Perot is also used as demodulator. Unlike the CO₂ generation beam, which is directly coupled to the inspected part, the beam from the detection laser and the collected beam scattered by the surface are transmitted by optical fibers.

If much larger areas have to be inspected or for complete flexibility of access all around a given stationary part, the generation unit that houses essentially the generation laser could be mounted at the end of the arm of a gantry robot (with 3 translation axis and one rotation axis in addition of the optical scanning mirror). Such a system has been implemented by UltraOptec for the US Air Force McClellan base and its configuration is sketched in figure 21 ⁹⁰. This system was thoroughly tested and its capability to inspect many parts of various shapes, materials and surface conditions was validated ⁹¹. The results obtained with the system were confronted with those obtained by conventional ultrasonics. The conclusion reached was a definite advantage of this laser-ultrasonic system over conventional ultrasonics for the inspection of contoured parts, but a lower throughput for parts essentially flat, which can be rapidly inspected by multiple conventional transducers in parallel. However, due the closure of the McClellan base, this system is not in operation anymore.

The systems presently in use at Lockheed Martin while having several distinguishing features with respect to the system installed for the US Air Force make however use of the same concept of a generation unit mounted on a gantry robot ⁸⁹.

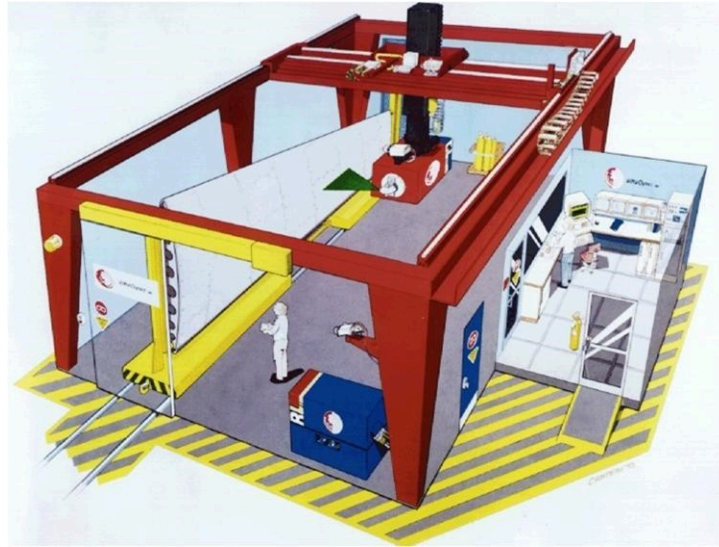


Figure 21. Sketch of the system implemented for the McClellan US Air Force base.

In addition to the use at Lockheed Martin, such a technology has been also used at validation and pre-production stages by aerospace companies in Europe using a system assembled by UltraOptec⁹² and a system made by the companies Iphoton and Tecnatom⁹³. In this system, a large articulated robot mounted on a linear translation platform was used to position the inspection head with its optical scanner head while the CO₂ beam, which in practice cannot be transmitted by an optical fiber, was transmitted by an articulated arm. This system is not anymore in operation but building upon the experience developed by building and using it, a system assembled by Tecnatom, which includes an optical scanner and a directly coupled CO₂ laser beam, while the inspected part is positioned by an articulated robot, has entered production use⁹⁴.

Since the fuselage of modern airplanes is made in long barrel sections by automatic fiber placement NRC with Tecnar has implemented the system pictured in figure 22, which allows inspection from inside the fuselage⁹⁵. In this system, the inspection head with its optical scanner is mounted at end of a long cantilever beam solidly anchored to the plant floor. As shown in figure 22, the CO₂ laser is located on top of the anchoring pivot. The scanner includes a single oscillating mirror mounted on a turret in such a way to allow 360 degrees inspection around the barrel. The scanner is also mounted on a pivot to allow inspection of the cockpit area and the longitudinal or circumferential stiffeners,

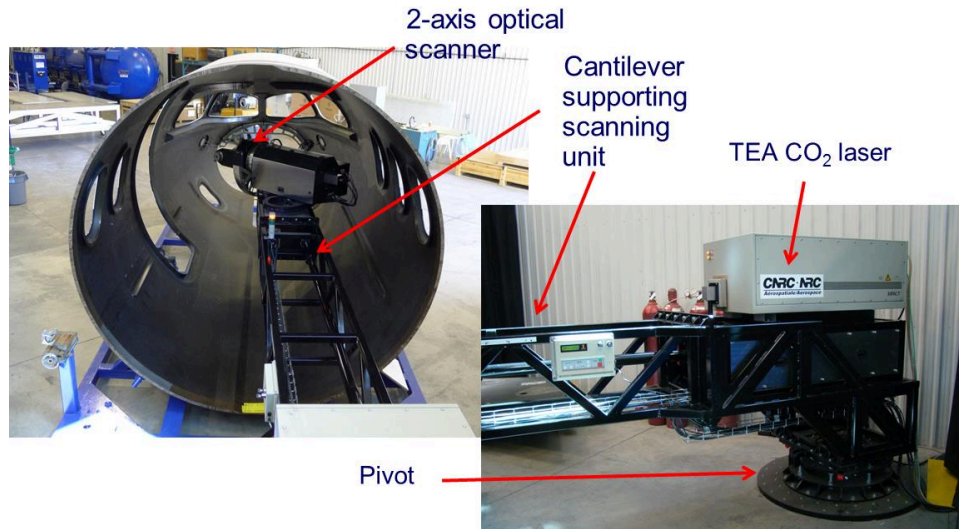


Figure 22: pictures of the system developed by NRC and Tecnar for fuselage inspection

In the case of composites, there is always efficient generation, whether the surface is rough or shiny or mirror-like. Such surfaces are often found from the tool side of the part or if the part has been made by Resin Transfer Molding (RTM). In this case mirror-scanning is inappropriate and the beam collected from the surface could quickly vanish to zero even when slightly off the normal direction. The solution is to mount the inspection head on a robot which orients the beams perpendicular to the surface. The robot trajectory is determined from the surface profile obtained by optical profilometry or CAD file of the part. NRC has developed a first generation of such an approach in which the CO₂ laser beam is guided by an articulated arm⁹⁶. Figure 23 show the inspection results obtained on composite panel with stiffeners (or stringers).

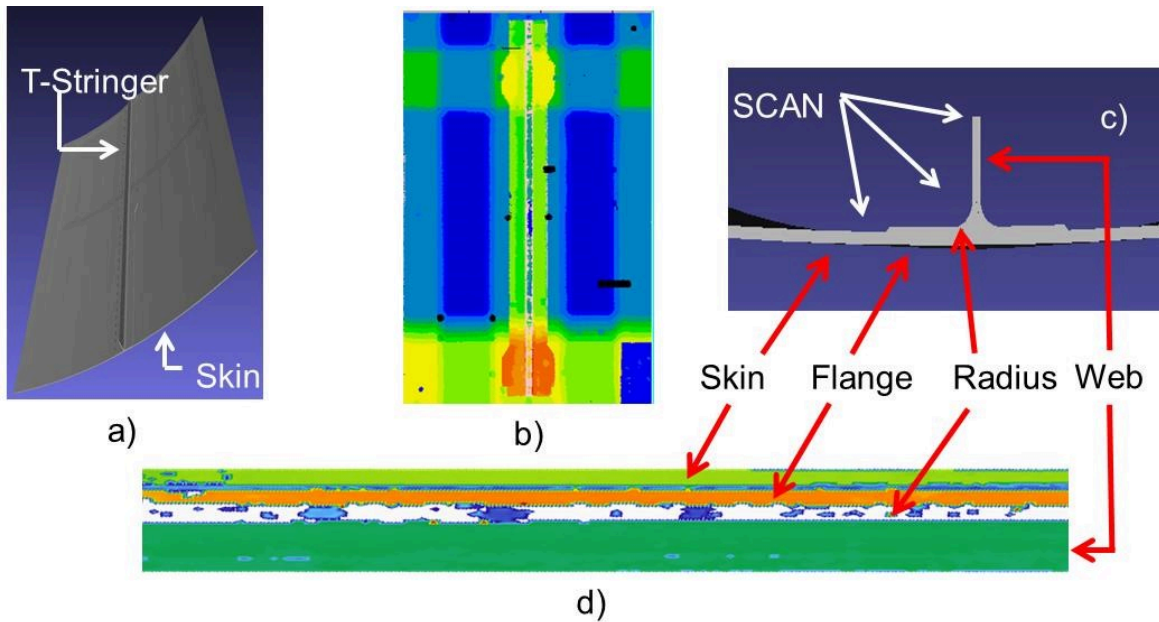


Figure 23: inspection around a T-stringer made by the robotic laser ultrasonic inspection system at NRC; the direction of the generation and detection laser beams is given by the robot; a) Picture of the panel with the T stringer; b) C-scan from the side opposite to the stringer; c) Sketch of the cross section of the stringer with sketch of the angular scan; d) C-scan over the stringer following linear and angular scanning and showing many flaws in the radius area.

NRC has also demonstrated that this technology could be used not only for inspecting fabricated parts but also for inspecting an aircraft during a maintenance operation. Figure 24 shows the laser-ultrasonic C-scan image of the horizontal stabilizer of a CF-18 airplane. Inspection was performed with no surface preparation in a maintenance hangar on a plane in flying conditions^{97,98}.

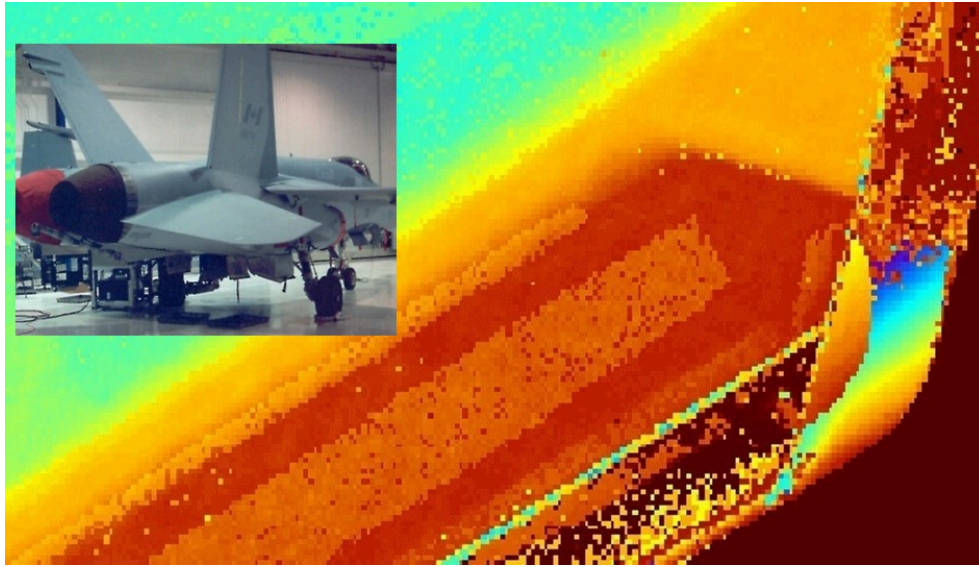


Figure 24. Laser-ultrasonic C-scan image of part of the horizontal stabilizer of a CF-18 airplane in undismantled and ready for take-off conditions. One will notice that, unlike conventional water jet ultrasonics, laser-ultrasonic allows scanning to the very edge of the part.

As previously mentioned the generated ultrasonic displacement is very broadband and in particular could be used to put in vibration any layer detached from the part. These vibrations are typically below 1 MHz and require for detection the use of a photorefractive interferometer. This approach (we call it laser tapping by similarity with the well known tap test) is particularly useful for detecting the detachment of a skin from an honeycomb or foam core. Figure 25 shows the results of the inspection test performed using this technique of a Nomex honeycomb part that has been damage by impact. As it can be seen the skin detachment is detected either from the impacted side or the opposite side.

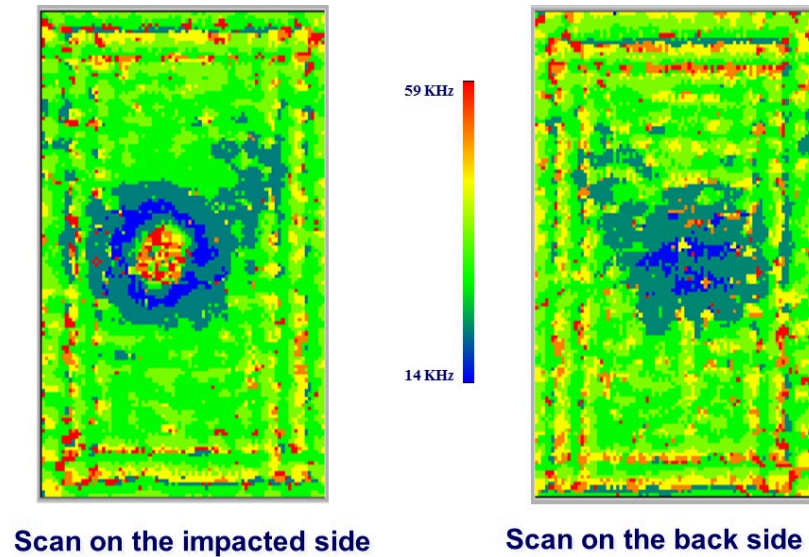


Figure 25: Laser tapping results (plot of the observed vibration frequency) from an impacted honeycomb panel (0.2 inch core spacing, 0.75 mm thick skin); as expected the indications from the 2 sides are mirror images.

5.2.2 Detection of cracks and other flaws in metals

Laser-ultrasonics can be applied to the detection of various flaws in metals such as pores or cracks. The signature of a crack is the largest when the crack opens to the surface opposite to generation and when the ultrasonic wave is emitted at an angle (by using the thermoelastic or ablation mechanism). In this case the crack and the part surface make a corner reflector which, particularly if the crack is approximately perpendicular to the surface, reflects back the incident wave upon the generation location.

In general to obtain a strong signature of a flaw one has to focus the wave onto the flaw. As mentioned above, this can be done by using SAFT. This processing technique has been applied in particular to the imaging of stress corrosion cracks in steel. One example of the results obtained is shown in figure 26 where the crack opening image of stress corrosion cracks in a stainless steel test sample is compared with the image obtained conventionally by liquid penetrants ⁹⁹.

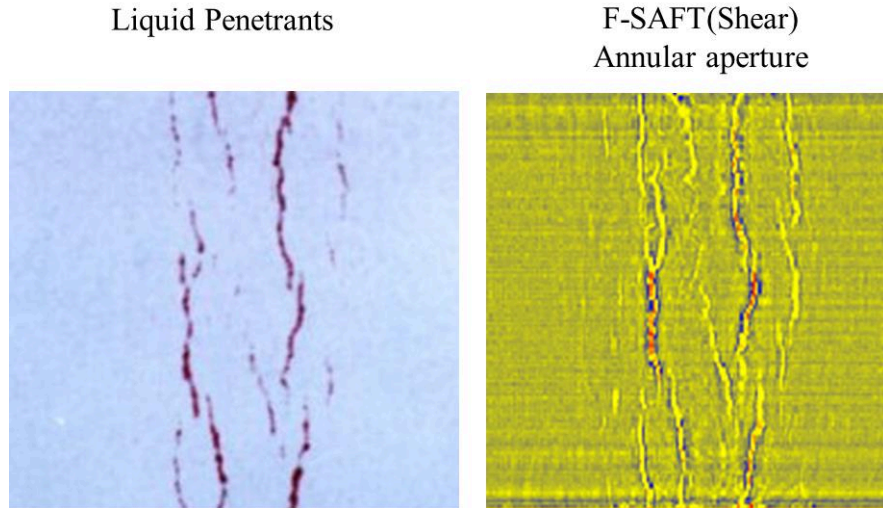


Figure 26. Comparison of crack opening images obtained by liquid penetrants (left) and laser-ultrasonic F-SAFT processing using shear waves and an annular aperture (right). The color code used in the image at right is indicative of the crack depth.

Another example of laser ultrasonics combined with SAFT is the detection of defects produced by friction stir welding (FSW). Laser ultrasonics has the advantage, particularly in the case of aluminum alloys in which ultrasonic scattering is weak, to generate very high frequencies: see figure 27 which compares the performance of laser ultrasonics with high frequency immersion ultrasonics (the performance of phase-array ultrasonics would have been even worse since phase-array transducers are typically limited to 15 MHz)¹⁰⁰. Laser ultrasonics has also been shown to be the best technique to detect incomplete weld penetration that does not pass a bending test¹⁰¹. The technique being non-contact and nor very sensitive to the roughness left on the surface by the tool has the potential to be used during the welding process, the part still being clamped to the machine. In this case if any flaw is found the weld could be reworked.

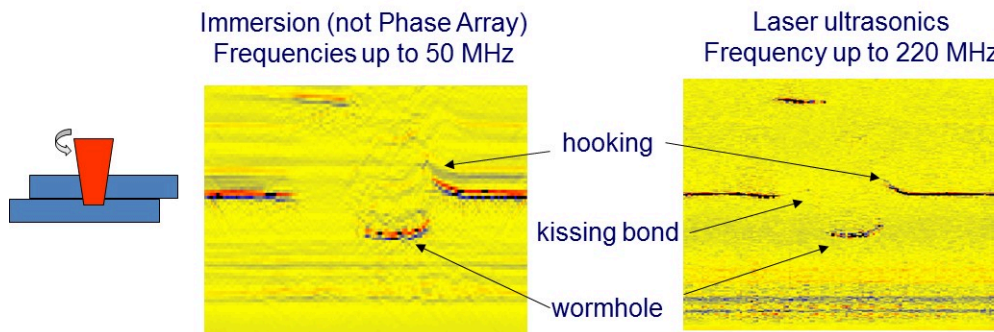


Figure 27: inspection of a lap FSW joint: comparison of immersion ultrasonics SAFT with laser ultrasonic SAFT.

Laser ultrasonics could be also very useful for multipass welds by allowing the detection of flaws after each pass or during welding. It has been implemented in the assembly of very thick hollow shafts by arc

welding in a production environment ¹⁰². We present in figure 28 results related to the same application, which show the detection artificial defects simulating lack of fusion along the weld preparation in a partial weld. This partial weld was inspected from the weld bead surface which has an undefined shape. To apply SAFT the surface profile of the bead was measured by laser triangulation ¹⁰³.

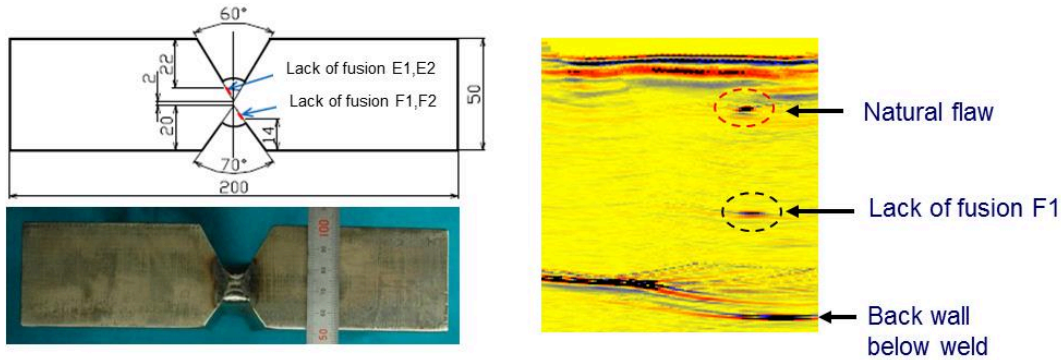


Figure 28: Inspection by laser ultrasonics plus SAFT of a partial weld. The part thickness is 50mm. Artificial defects simulating lack of fusion are 3 (height) x 16 mm (along the weld). B-scan across flaw F1 has been corrected for top surface profile of the weld bead. Scan length transverse to the weld is 13 mm.

An other example of weld inspection right over the weld bead, which is not possible with conventional ultrasonics, is the inspection of the fillet weld making a lap joint between 2 parts shown in figure 29 ¹⁰⁴. This weld was part of an automotive suspension frame. Weld penetration is well detected as shown by the metallographic observation after sectioning. The shape of the weld bead was measured by laser triangulation using the detection laser beam for illumination. A special algorithm based on ultrasonic attenuation was developed for evaluating the depth of the fused zone.

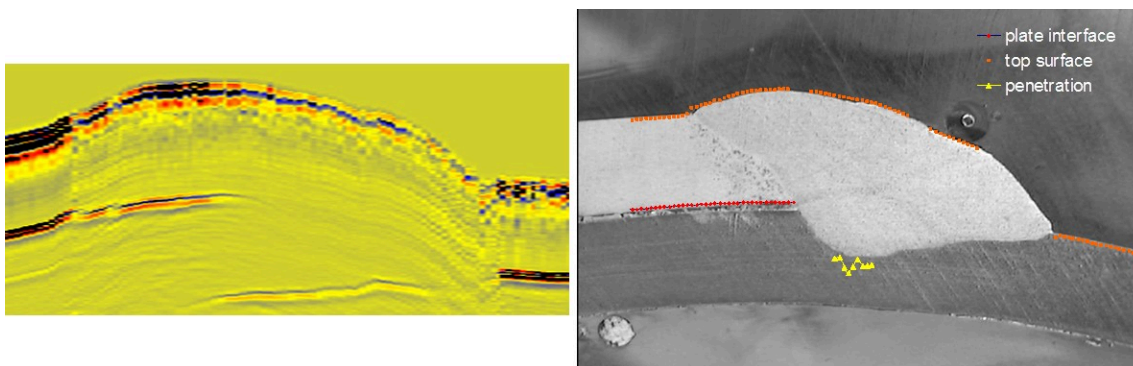


Figure 29: Laser ultrasonic inspection of an automotive suspension frame fillet weld. Left: laser ultrasonic image combined with optical profilometry of the bead surface. Right: Metallographic image obtained after sectioning the weld with superimposed in red and yellow results derived from profilometry and laser-ultrasonics.

Additive manufacturing is an emerging technology which is expected to revolution the whole sector of manufacturing. In the case of metallic structural parts, which are made by fusing powders or wires with a laser or an electron beam, this technology is not ready yet to replace conventional manufacturing technologies since the requirements for part quality is very high, regarding dimensions, shape, the presence of flaws (porosity, cracks), mechanical properties, microstructure ... Laser ultrasonics by its characteristics (non-contact, complex shape, broad band ..) has the potential to be a useful technology for process development and in-process or after-process part inspection. We present in figure 30 an inspection result obtained off-line on a test specimen made by Inconel powder laser deposition¹⁰⁵. This result has been validated by x-ray micro-CT inspection. Experimentation on this application is also being performed elsewhere¹⁰⁶.

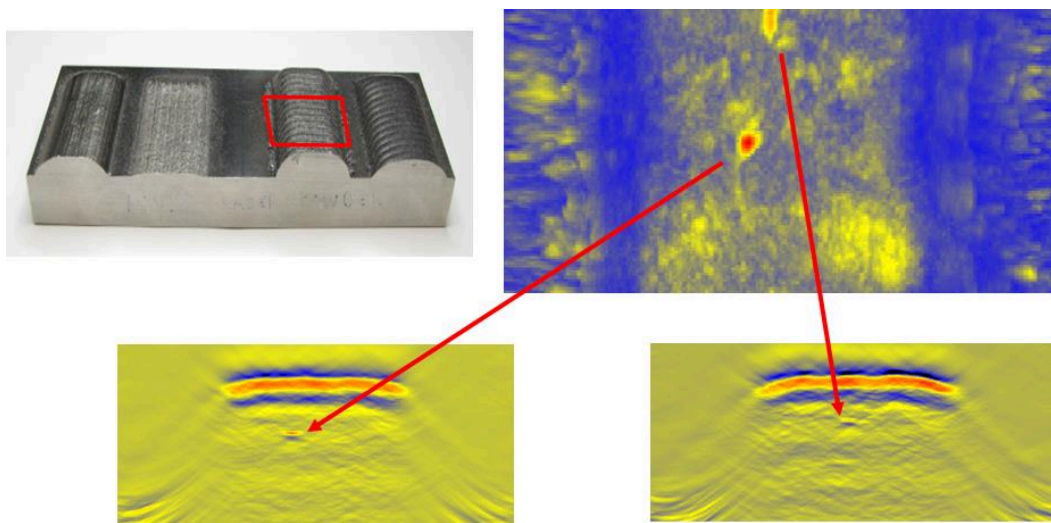


Figure 30: Application of laser ultrasonics to additive manufacturing; upper left: picture of the Inconel test specimen with the scan zone 25x10 mm (0.1 mm steps) indicated in red; upper right: C-scan; lower left and right : B-scans extending from the top of deposition to 7 mm below and across the 2 identified flaws.

5.3. Material characterization

As mentioned above, material microstructure affects ultrasonic velocity, attenuation and causes scattering and anisotropy. Laser ultrasonics which is non-contact is particularly useful for microstructure characterization at elevated temperatures. In particular laser-ultrasonics can monitor austenitic grain growth by using a model that describes the effect of grain size on attenuation^{107,108}. Figure 31 shows an example of this “laser-ultrasonics metallography”, in which grain size determined by analysis of ultrasonic attenuation and grain size measured by conventional metallography after quenching are compared. This data was obtained by heating the steel sample in a GleebleTM thermo-mechanical simulator. Such a system in which laser-ultrasonics is coupled to the thermo-mechanical simulator has been commercially developed¹⁰⁹. Figure 32 shows the prototype of such a system available at NRC. Austenitic grain size measurement was also demonstrated on-line on seamless tubes at Timken under

contract from the US Department of Energy using the system developed for wall thickness measurement. Figure 33 shows the excellent correlation between the austenitic grain size measured by quenching, polishing, etching and metallographic examination on pieces cut from tubes and the values provided by laser-ultrasonics ⁷⁵.

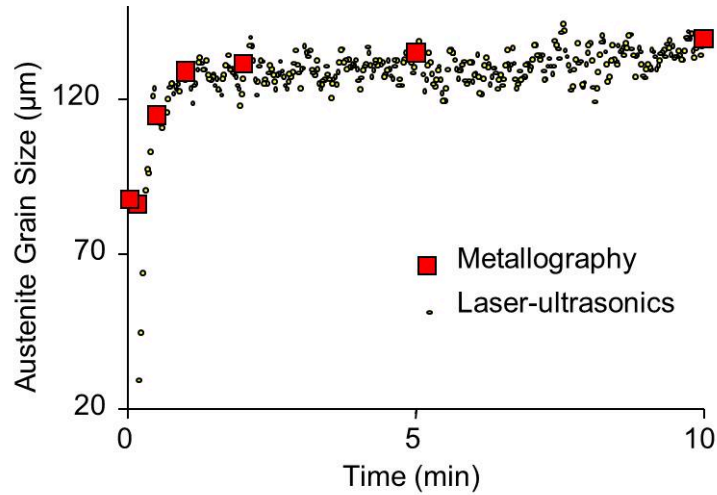


Figure 31. Laser-ultrasonic “metallography”



Figure 32: Laser-ultrasonics coupled to a Gleeble TM 3500 thermo-mechanical simulator

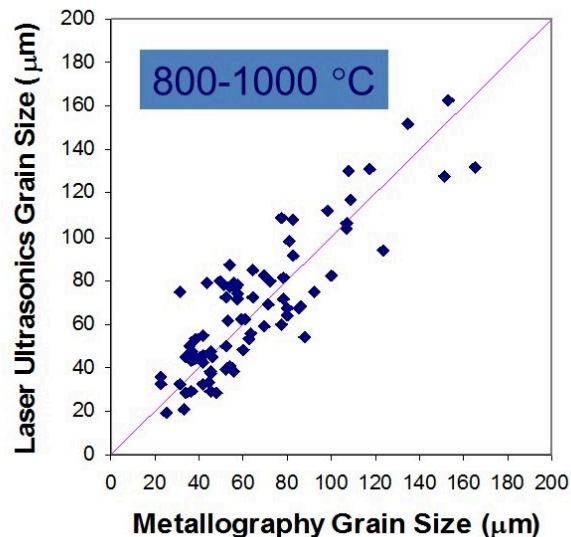


Figure 33: On-line measurement of austenitic grain size: comparison between the values obtained by laser-ultrasonics and conventional metallography.

Another application of laser-ultrasonics to the steel industry is the monitoring of phase transformation, such as the transformation of austenite into ferrite, by the sensitivity of ultrasonic velocity to phase fraction^{110,111,112,113}. It has been in particular used for measuring the retained austenite fraction in TRIP or other multiphase steels¹¹⁴. Laser-ultrasonics could also be applied to monitoring and quantifying austenite decomposition¹¹⁵. It has also been demonstrated to be able to monitor annealing and recrystallization of steel by following the change of ultrasonic velocity^{116,117}. The measurement of grain orientation (steel texture) has been demonstrated either by generating and detecting surface or plate waves launched in various directions or using an ultrasonic spectroscopy technique in which the initial launched longitudinal wave is converted by diffraction after multiple reflections into shear waves with different polarizations¹¹⁸. The application to the annealing of aluminum alloys has also been explored¹¹⁹ and was the object of an on-line experimentation by NRC¹²⁰.

Under support of the American Iron and Steel Institute, NRC has also performed experiments on a steel strip finishing line with the purpose of measuring mechanical properties (tensile strength, yield strength ...) ¹²¹. This is possible since these properties are function of steel microstructure, which can be sensed with ultrasound, while assuming that the steel composition is known. Currently, under support from European Commission funding, a prototype sensor for on-line laser ultrasonic sensing during hot rolling of steel is being developed and tested¹²². Such a sensor is expected to allow improving hot rolling mill productivity by monitoring grain growth and recrystallization.

5.4 Laser shockwave testing

As mentioned in the introduction, lasers can be used to produce very high stresses in materials (shockwaves). These stresses are generated as compressive and rely on the production of a plasma which

is confined by some other material transparent to the laser (water is often used). Confinement of the produced plasma causes a very high pressure. When the compression wave encountered a free boundary it is converted to a tensile wave. This effect is used to tensile test the material to evaluate its cohesion strength¹²³. It is also used to test the adhesion of coatings¹²⁴ or adhesive bonds^{125,126}. Figure 34 show the principle of this shockwave testing of adhesive bonds. Such a technique can be applied on an adhesively bonded structure following calibration to determine the suitable pressure or laser energy to apply. If the bond passes the test, i.e. the bond is not broken, it is then above a predetermined and acceptable strength, as determined by calibration, otherwise it is too weak and the part should be rejected. Bond breakage is verified by ultrasonic inspection (conventional or preferably laser-ultrasonics). This technique is much better than the one consisting to perform mechanical testing on coupons which may not be representative of the actual conditions of the bonded surfaces on the part (they could be for example contaminated). A first generation of a bond testing system in which disbonding is detected by an EMAT has been developed¹²⁷. This bond testing technique is unique since there is no other reliable technique to tensile proof test adhesive bonds nondestructively, but it requires a very high energy laser (10 J and above).

Real time diagnostic can be performed during the test by monitoring the back surface velocity. Although another interferometric system developed for shockwave physics can be used¹²⁸, NRC has developed a velocimeter based on a solid planar Fabry-Perot etalon that uses as laser source the one developed for laser-ultrasonics¹²⁹. Using this approach, an integrated bond testing system that comprises the laser for producing the shock and post-shock laser-ultrasonic inspection has been integrated. This system is currently used for the development a new nuclear fuel for safe operation of high neutron flux reactors based on the encapsulation of low-enrichment uranium between aluminum foils¹³⁰.

Figure 35 shows the application of the technique to testing adhesive bonds between carbon-epoxy composites¹³¹. Two 8-ply carbon-epoxy laminates were adhesively bonded with a two-part adhesive modified for weaker strength and were shock-loaded with increased laser energy. All normalized velocimeter signals get approximately superimposed except when breakage occurs, which is revealed by an upturn in the traces. The laser energy at which this upturn occurs is the threshold loading. Breakage is actually verified by post-shock laser ultrasonic inspection. Using experimental data such as the one shown in figure 35 and velocimeter calibration, modelling has been developed to get the value of the threshold breaking stress as well as the location of breakage.

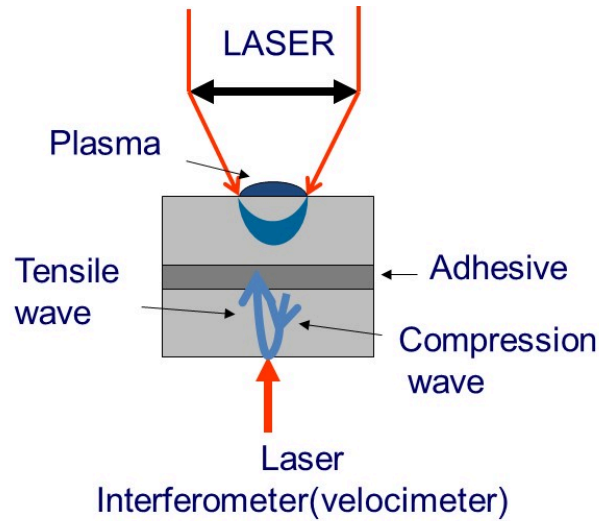


Figure 34: Principle of bond testing by laser induced shockwave.

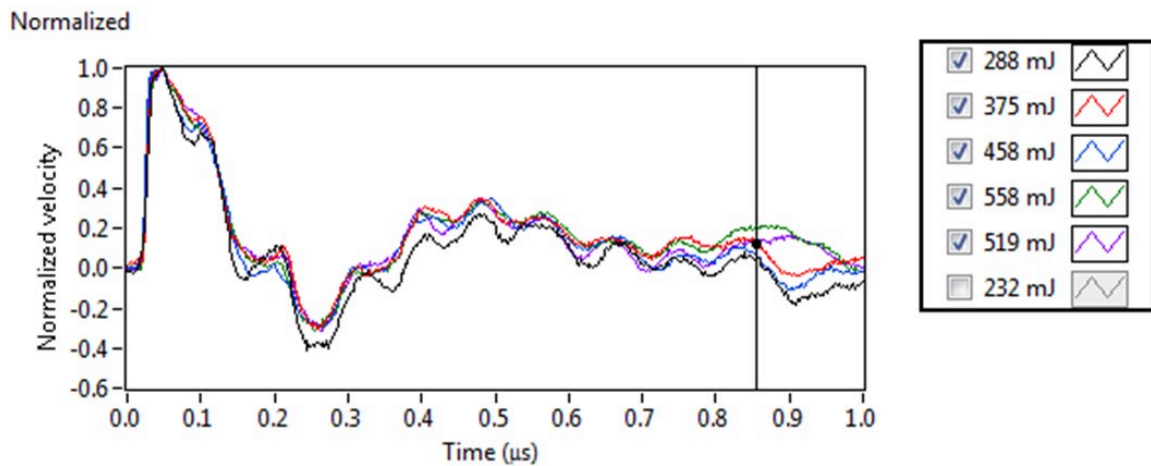


Figure 35: Example of velocimeter recording on a bonded laminate (8-ply to 8-ply carbon-epoxy with a two-part adhesive modified to get weaker strength); the laser energy is progressively increased until breakage occurs.

5.5 Other applications

Other applications of laser-ulasonics that have been explored include the detection of degradation of metallic structures, such as fatigue cracking¹³² and corrosion thinning in aluminum airframes¹³³. The technique has also shown good potential for measuring on-line the mechanical properties of a paper web and its tension^{134,135,136}. The measurement of the thickness of an oil spill from an airplane is also another but challenging application which has been demonstrated^{137,138}. The detection of defects at a smaller scale (e.g. on chips or electronic boards) has also been explored and is an application well adapted to laser-ulasonics by the capability of the technique to provide high frequency ultrasonic testing without water

coupling¹³⁹. A field prototype of a laser ultrasonic system for inspecting concrete structures, including in particular those in transportation tunnels, has also been developed¹⁴⁰.

Regarding stress measurement, which is challenging since the effect of stress on ultrasonic velocity is small, particularly in comparison to the anisotropy produced by grain orientation, laser-ultrasonics has been explored for the measurement of the compressive stress produced by shot peening or laser peening and its through-depth distribution¹⁴¹. By detecting the surface skimming wave generated at the same time as the Rayleigh surface and measuring their propagation times, the technique has also shown good potential to be practically used for the measurement of thermal stress in rails¹⁴². Convincing results have also been obtained for the measurement of residual stress in FSW of aluminum alloys¹⁰⁰.

6. Summary and conclusion

We have presented a broad overview of the basics and of the various technological aspects of laser-ultrasonics. We have outlined the various principles and discussed the phenomena involved in laser generation and detection. We have also presented the advantages and drawbacks of this technique, particularly in comparison with conventional piezoelectric-based ultrasonics. Several of those are linked to the basic characteristic of laser-ultrasonics, which is the use of light as a means for ultrasound generation and detection. Light allows ultrasonic testing without contact and at a distance, thus making possible a wide range of high temperature applications, but sensitivity is on the other hand dependent upon the number of detected photons, which in turn could require a special high power laser for detection (unless the surface has good reflection properties, which is usually the case for microelectronic applications). Many advantages and drawbacks of laser-ultrasonics are also linked to the fact that the material is actually the emitting transducer. This distinguishing feature allows probing more easily parts with complex shapes, but may lead to several limitations depending upon the material, such as very weak emission or material damage. In this regard, we have outlined ways that have been devised to increase the emitted ultrasonic wave amplitude for a specific configuration or task. Detection interferometers well adapted to industrial applications have also been described, including the confocal Fabry-Perot and the two-wave mixing photorefractive interferometer.

Another feature of laser-ultrasonics that has been noted is the complexity of the technique that includes usually two lasers and a detection interferometer. This makes it generally a high cost solution, but in spite of that, it turned out to be cost effective for several applications. The few that have ended up at the time of this writing into commercial sensors have been described: the inspection of polymer-matrix composites, the wall thickness measurement of hot steel tubes during processing and the thickness measurement and characterization of thin layers in microelectronics by two different approaches.

Many other applications have been explored in the laboratory and several have been the object of demonstration prototypes or even of a first generation of commercially available systems with potential of broader deployment.

In view of the increasing automation of manufacturing, based on extensive use of robotics, sensors, digital means and artificial intelligence (Smart Industry or Industry 4.0), laser ultrasonics that allows 'viewing' inside parts is expected to find broader use within this industrial revolution. In fact, laser ultrasonics goes much beyond any vision-based sensor which provides only information on shape and surface conditions. It could also be relatively easily combined with vision systems since both technologies are based on optics, and in this way to get a sensing system providing complete information on a manufactured object from its surface to deep inside. Laser ultrasonics is also unique by providing without contact, and even remotely, information on the presence of flaws in a manufactured part and information on its microstructure, which both relate to the part actual mechanical properties. Since this sensing is

without contact and generally independent of part shape and surface orientation, laser-ultrasonics could be applied during processing, thus providing information on the process and allowing detection early-on of flaws in manufactured parts and process deviation. As such, in spite of its complexity and cost, this technique is expected to be found cost effective for use in the factory of the future.

References

1. Maiman, T. H., *Nature*, **187**, 493 (1960).
2. White, R. M., "Generation of elastic waves by transient surface heating", *J. Appl. Phys.*, **34**, 3559 (1963).
3. Askar'yan, A., Prokhorov, A. M., Chanturya, G. F., Shipulo, M. P., "The effect of a laser beam in a liquid", *Sov. Phys. JETP*, **17**, 1463 (1963).
4. Scruby, C.B. and Drain, L.E., *Laser-Ultrasonics: Techniques and Applications*, Adam Hilger, Bristol, UK (1990).
5. Hutchins, D. A., "Ultrasonic generation by pulsed lasers", in *Physical Acoustics*, vol. 28, eds. W. P. Mason and R. N. Thurston, Academic Press, New-York, 1988, p. 21.
6. Dewhurst, R.J., Hutchins, D.A., Palmer, S.B. and Scruby, C.B., "Quantitative measurements of laser-generated acoustic waveforms", *J. Appl. Phys.* **53**, 4064 (1982).
7. Rose, L.R.F., "Point-source representation for laser-generated ultrasound", *J. Acoust. Soc. Am.*, **75**, 723 (1984).
8. Doyle, P.A., "On epicentral waveforms for laser-generated ultrasound", *J. Phys.D: Appl. Phys.* **19**, 1613 (1986).
9. Scruby, C.B., Dewhurst, R.J., Hutchins, D.A. and Palmer, S.B. "Laser generation of ultrasound in metals", in *Research techniques in Nondestructive testing*, vol. 5, chapter 8, edited by R. S. Sharpe, Academic press, New-York, p. 281.
10. Vogel, J. A., Bruinsma, A. J. A., *Non-destructive testing*, vol.4, eds. J. M. Farley and R. W. Nicols, Pergamon, Oxford, 1988, p. 2267.
11. Noroy, M.-H., Royer, D., Fink, M., "Transient elastic wave generation by an array of thermoelastic sources", *Appl. Phys. Lett.*, **63**, 3276 (1993).
12. Wang, X., Littman, M. G., McManus, J. B., Tadim M., Kimm Y. S., Askarm A., Rabitzm H., "Focused bulk ultrasonic waves generated by ring-shaped laser illumination and application to flaw detection", *J. Appl. Phys.*, **80**, 4274 (1996).
13. Monchalain, J.-P., Choquet, M., Héon, R., Bouchard, P., Padioleau, C., Dubois, M., Enguehard, F., Bertrand, L., Sturrock, W. R., McRae, K. I., "Application of Laser-Ultrasonics to the Inspection of Composite Materials", Proceedings of the *2nd Canadian International Composites Conference (Cancom '93)*, Sept. 27-29, Ottawa, Ont., eds W. Wallace, R. Gauvin and S. V. Hoa, Canadian Association for Composite Structures and Materials, Montreal, 1993, p. 501.
14. Telshow, K. L., and Conant, R. J., "Optical and thermal parameters effects on laser-generated ultrasound", *J. Acoust. Soc. Am.*, **88**, 1494 (1990).
15. Dubois, M., Enguehard, F. and Bertrand, L., "Analytical one-dimensional model to study the ultrasonic precursor generated by a laser", *Phys. Rev. E*, **50**, 1548 (1994).
16. McDonald, F. A., "Practical quantitative theory of photoacoustic pulse generation", *Appl. Phys. Lett.*, **54**, 1504 (1989).
17. Dubois, M., Enguehard, F., Bertrand, L., Choquet, M., Monchalain, J.-P., " Modeling of laser thermoelastic generation of ultrasound in an orthotropic medium", *Appl. Phys. Lett.*, **64**, 554 (1994).
18. Dubois, M., Enguehard, F., Bertrand, L., Choquet, M., Monchalain, J.-P., "Numerical and experimental studies of the generation of ultrasound by laser", 8th International Topical Meeting on Photoacoustic and Photothermal Phenomena, Pointe-à-Pitre, Guadeloupe, Jan. 22-25 1994, *J. Physique IV*, Colloque C7, vol 4, p.689, (1994).
19. Hutchins, D. A., Dewhurst, R. J. and Palmer, S. B., "Laser generated ultrasound at modified metal surfaces", *Ultrasonics*, **19**, 103 (1981).
20. Arnold, W., Betz, B. and Hoffman, B., "Efficient generation of surface acoustic waves by thermoelectricity", *Appl. Phys. Lett.*, **47**, 672 (1985).
21. Scala, C. M. and Doyle, P. A., "Time- and frequency-domain characteristics of laser-generated ultrasonic surface waves", *J. Acoust. Soc. Am.*, **85**, 1569 (1989).
22. Aindow, A. M., Dewhurst, R. J. and Palmer S. B., "Laser generation of directional surface acoustic wave pulses in metals", *Optics Com.*, **42**, 116 (1982).
23. Murray, T. W., Baldwin, K. C., Wagner, J. W., "Laser ultrasonic chirp sources for low damage and high delectability without loss of temporal resolution", *J. Acoust. Soc. Am.*, **102**, 2742 (1997).
24. Sharples, S. D., Clark, M., Somekh, M. G., "All-optical adaptive scanning acoustic microscope", *Ultrasonics*, **41**, 295 (2003).

25. Maldague, X., Cielo, P., Jen, C. K., "NDT applications of laser-generated focused ultrasonic waves", *Materials Evaluation*, **44**, 1120 (1986).
26. Yamanaka, K., Kolosov, O. V., Nagata, Y., Koda, T., Nishino, H. and Tsukahara, Y., "Analysis of excitation and coherent amplitude enhancement of surface acoustic waves by phase velocity scanning method", *J. Appl. Phys.*, **74**, 6511 (1993).
27. Hoffman, A. and Arnold, W., "Calculation and measurement of the ultrasonic signals generated by ablating material with a Q-switched pulse laser", *Appl. Surface Science*, **96**, 71 (1996).
28. Hoffman, A. and Arnold, W., "Modeling of the ablation source in laser-ultrasonics", in *Review of Progress in Quantitative Nondestructive Evaluation*, vol. 19A, eds. D. O. Thompson and D. E. Chimenti, Plenum, New-York, 2000, p. 279.
29. Hébert, H, Vidal, F., Martin, Kieffer, J.-C., Nadeau, A., Johnston, T.W., Blouin, A., Moreau, A. and Monchalin, J.-P. "Ultrasound generated by a femtosecond and a picosecond laser pulse near the ablation threshold", *J. Appl. Phys.*, **98**, 033104 (2005).
30. Murray, T. W. and Wagner, J. W., "Laser generation of acoustic waves in the ablative regime", *J. Appl. Phys.*, **85**, 2031 (1999).
31. Monchalin, J.-P., "Optical detection of ultrasound", *IEEE Trans. Sonics, Ultrasonics*, Freq. Control, **UFFC-33**, 485 (1986).
32. Dewhurst, R. J. and Shan, Q., "Optical remote measurement of ultrasound", *Meas. Sci. Technol.*, **10**, R139 (1999).
33. Blouin, A., Delaye, P., Drolet, D., de Montmorillon, L.-A., Launay, J.-C., Roosen, G. and Monchalin, J.-P., "Optical detection of ultrasound using two-wave mixing in semiconductor photorefractive crystals and comparison with the Fabry-Perot", in *Nondestructive Characterization of Materials VIII*, Proceedings of the conference, Boulder, Colorado, June 15-20, 1997, eds. R. E. Green Jr. and C.O. Ruud, Plenum Press, NY, 1998, p. 13.
34. Caves, C. M., "Quantum-mechanical noise in an interferometer", *Phys. Rev D*, **23**, 1693 (1981).
35. Pouet, B., Breugnot S. and Clemenceau, P., "An Innovative Interferometer for Industrial laser Ultrasonic Inspection", in *Review of Progress in QNDE*, vol. 24A, eds. D.O. Thompson and D.E. Chimenti, AIP Conference Proceedings, New-York, 2005, p. 273.
36. Pouet, B., Breugnot S. and Clemenceau, P., "Recent Progress in Multi-Channel Quadrature Interferometer: Demonstration of a Compact Fiberized Architecture", in *Review of Progress in QNDE*, vol. 26, eds. D.O. Thompson and D.E. Chimenti, AIP Conference Proceedings, New-York, 2007, in press.
37. Kaule, W., in Proceedings of 8th World NDT conference, Cannes, France, paper 3J5, 1976.
38. Connes, P., "L'étalon de Fabry-Pérot sphérique", *J. Physique et le Radium*, **19**, 262 (1958).
39. Monchalin, J.-P., and Héon, R., "Laser ultrasonic generation and optical detection with a confocal Fabry-Perot interferometer", *Materials Evaluation*, **44**, 1231 (1986).
40. Shan, Q., Bradford, A. S. and Dewhurst, R. J., "New field formulas for the Fabry-Perot interferometer and their application to ultrasound detection", *Meas. Sci. Technol.*, **9**, 24 (1998).
41. Monchalin, J.-P., Héon, R., Bouchard, P., Padioleau, C., "Broadband optical detection of ultrasound by optical sideband stripping with a confocal Fabry-Perot", *Appl. Phys. Lett.*, **55**, 1612 (1989).
42. Monchalin J.-P. and Héon, R., "Laser optical ultrasound detection using two interferometer systems", US patent No 5,080,491 (14 Jan. 1992).
43. Blouin, A., Padioleau, C., Néron, C., Lévesque, D. and Monchalin J.-P., "Differential Confocal Fabry-Perot for the Optical Detection of Ultrasound", in *Review of Progress in QNDE*, vol. 26, eds. D.O. Thompson and D.E. Chimenti, AIP Conference Proceedings, New-York, 2007, in press.
44. Ing, R. K., Monchalin, J.-P., "Broadband optical detection of ultrasound by two-wave mixing in a photorefractive crystal", *Appl. Phys. Lett.* **59**, 3233 (1991).
45. Blouin, A., Monchalin, J.-P., "Detection of ultrasonic motion of a scattering surface by two-wave mixing in a photorefractive GaAs crystal", *Appl. Phys. Lett.*, **65**, 932 (1994).
46. Delaye, P., Blouin, A., Drolet, D., de Montmorillon, L.-A., Roosen, G., Monchalin, J.-P., "Detection of an ultrasonic motion of a scattering surface by photorefractive InP:Fe under an applied DC field", *J. Opt. Soc. Am.*, **14**, 1723 (1997).
47. de Montmorillon, L.-A., Biaggio, I., Delaye, P., Launay, J.-C., Roosen, G., "Eye-safe large field-of-view homodyne detection using a photorefractive CdTe:V crystal", *Opt. Comm.* **129**, 293 (1996).
48. Drolet, D., Néron, C., Blouin, A. and Monchalin, J.-P., "Specifications of an ultrasonic receiver based on two-wave mixing in photorefractive gallium arsenide implemented in a laser-ultrasonic system", in *Review of Progress in QNDE*, vol. 15, eds. D.O. Thompson and D.E. Chimenti, Plenum, New-York, 1996, p. 637.
49. P. Delaye, A. Blouin, L.-A. de Montmorillon, D. Drolet, J.-P. Monchalin, G. Roosen, "Photorefractive detection of ultrasound", *Proc. SPIE*, **3137**, 171, (1997).

50. Campagne, B., Néron, C., Blouin, A. and Monchalain, J.-P., "Doppler frequency-shift compensated photorefractive interferometer for ultrasound detection on objects in motion", in *Review of Progress in QNDE*, vol. 22A, eds. D.O. Thompson and D.E. Chimenti, AIP Conference Proceedings, New-York, 2003, p. 273.
51. Murray, T. W. and Krishnaswamy, S., "Multiplexed interferometer for ultrasonic imaging", *Opt. Eng.*, **40**, 1321 (2001).
52. Grappin, F., Delaye, P. and Roosen, G., "Parallel processing of ultrasonic signals in a single photorefractive crystal", Proceedings of the 9th conference on *Photorefractive Effects, Materials and Devices*, La colle sur Loup, France, June 17-21, 2003, *Trends-in-Optics-and-Photonics*, Optical Society of America, Washington DC, vol. 87, p. 463.
53. Hale, T. C., Telschow, K. L. and Deason, V. A., "Photorefractive optical lock-in vibration spectral measurement", *Appl. Optics*, **36**, 8248 (1997).
54. Telschow, K. L., Deason, V. A., Schley, R. S. and Watson, S. M., "Direct imaging of traveling Lamb waves in plates using photorefractive dynamic holography", *J. acoust. Soc. Am.*, **106**, 2578 (1999).
55. Bowers, J.E., 'Fiber-optical sensor for surface acoustic waves', *Appl.Phys.Lett.* **41**,231 (1982).
56. Fomitchov, P. A., Krishnaswamy S. and Achenbach, J.D., 'Compact phase-shifted Sagnac interferometer for ultrasound detection', *Opt. Laser Tech.* **29**,333(1997)
57. Pelivanov, I., Bumac, T., Xia J., Wei, C-W. and O'Donnell, M. 'NDT of fiber-reinforced composites with a new fiber-optic pump-probe laser-ultrasound system', *Photoacoustics* **2**,63-74 (2014).
58. Stratoudaki T., Hernandez J., Clark M. and Somekh M. G., 'Cheap optical transducers(CHOTs) for narrowband ultrasonic applications', *Meas. Sci. Technol.* **18**, 843-851 (2007).
59. Stratoudaki, T., Clark, M. and Somekh, M.G., 'Cheap optical transducers (CHOTS) for generation and detection of longitudinal waves', *2012 IEEE International Ultrasonics Symposium*, pp. 961-964, 2012.
60. Monchalain, J.-P., "Progress towards the application of laser-ultrasonics in industry", in *Review of Progress in Quantitative Nondestructive Evaluation*, vol. 12, edited by D. O. Thompson and D. E. Chimenti, Plenum, New-York,1993, p. 495.
61. Kane, T.J. and Byer, R. L., "Monolithic unidirectional single-mode Nd:YAG ring laser", *Opt. Lett.*, **10**, 65 (1985).
62. Drake, T., Osterkamp, M., Yawn, K. And Do, T. , "Improved laser technology for Industrial Laser Ultrasonics", presented at *Review of Progress in QNDE*, Golden, Colorado, July 25-30, 2004, unpublished.
63. Blouin, A. and Monchalain, J.-P., "Optical amplification of the laser ultrasonic signal", in *Review of Progress in QNDE*, vol. 23, eds. D.O. Thompson and D.E. Chimenti, AIP Conference Proceedings, New-York, 2004, p. 270.
64. Carrion, L., Blouin, A., Padioleau, C., Monchalain J.-P., "Single-frequency pulsed laser oscillator and system for laser-ultrasonics", *Meas. Sci. Technol.*, **15**, 1939-1946 (2004).
65. Seydel, J.A., "Ultrasonic synthetic aperture focusing techniques in NDT", in *Research Techniques in Nondestructive Testing*, Vol. 6, ed. R. S. Sharpe, Academic, New-York, 1983.
66. Blouin, A., Lévesque, D., Néron, C., Drolet, D. and Monchalain, J.-P., "Improved resolution and signal-to-noise ratio in laser-ultrasonics by synthetic aperture focusing technique (SAFT) processing", *Optics Express* **2**, 531 (1998).
67. Lorraine, P. W., Hewes R. A. and Drolet, D., "High resolution laser ultrasound detection of metal defects", in *Review of Progress in Quantitative Nondestructive Evaluation*, vol. 16, eds. D. O. Thompson and D. E. Chimenti, Plenum Press, New-York, 1997, p. 555.
68. Mayer, K., Marklein, R., Langenberg, K. J. and Kreutter, T., "Three-dimensional imaging system based on Fourier transform synthetic aperture focusing technique", *Ultrasonics*, **28**, 241 (1990).
69. Busse, L. J., "Three-dimensional imaging using a frequency-domain synthetic aperture focusing technique", *IEEE Transactions UFFC* **39**, 174 (1992).
70. Lévesque, D., Blouin, A., Néron, C. and Monchalain, J.-P., "Performance of laser-ultrasonic F-SAFT imaging", *Ultrasonics*, **40**,1057 (2002).
71. Lorraine, P. W., "Laser ultrasonic imaging of Lamb waves in thin plates", in *Review of Progress in Quantitative Nondestructive Evaluation*, vol. 17, eds. D. O. Thompson and D. E. Chimenti, Plenum Press, New-York, 1998, p. 603.
72. Stratoudaki, T., Clark, M., Wilcox, P.D., 'Laser induced ultrasonic phased array using full matrix capture data acquisition and total focusing method' *Opt. Express* **24**, 21921-21938 (2016).
73. Monchalain, J.-P., Choquet, M., Padioleau, C., Néron, C., Lévesque, D., Blouin, A., Corbeil, C., Talbot, R., Bendada, A., Lamontagne, M., Kolarik II, R. V., Jeskey, G. V., Dominik, E. D., Duly, L. J., Samblanet, K. J., Agger, S. E., Roush, K. J., Mester, M. L., "Laser ultrasonic system for on-line steel tube gauging", in *Review of Progress in Quantitative Nondestructive Evaluation*, vol. 22A, eds. D. O. Thompson and D. E. Chimenti, AIP Conference Proceedings, New-York, 2003, p. 264.
74. Deppe, G. J., "Wall thickness measurement by laser UT on hot tubes in a rolling mill", *International Tube Association Conference*, Bilbao, Spain, Oct. 24-28, 2001; available from NDT.net (<http://www.ndt.net>), March 2002, vol. 7, No. 03.

75. Kruger, S., Lamouche, G., Monchalain, J.-P., Kolarik II, R. V., Jeskey, G., Choquet, M., "On-line Monitoring of Wall thickness and Austenitic Grain size of a Seamless I Tubing Production Line at The Timken Co.", *Iron & Steel technology*, Oct 2005, pp. 25-31.
76. <http://tecnar.com/lut-evolution>
77. Thomsen, C., Grahn, H. T., Maris, H. J. and Tauc, J., "Surface generation and detection of phonons by picosecond light pulses", *Phys. Rev. B.*, **34**, 4129 (1986).
78. Maris, H., "Picosecond Ultrasonics", *Scientific American*, p.86, Jan. 1998.
79. Morath, C. J., Collins, G. J., Wolf, R. G., Stoner, R. J., "Ultrasonic multiplayer metal film metrology", *Solid State Technology*, p.85, June 1997.
80. <http://www.rudolphtech.com>
81. Rogers, J.A., Fuchs, M., Banet, M.J., Hanselman, J.B., Logan, R. and Nelson, K.A., "Optical system for rapid materials characterization with transient grating technique: Application to nondestructive evaluation of thin films used in microelectronics", *Appl. Phys. Lett.*, **71**, 225 (1997).
82. Rogers, J.A., Maznev, A.A., Banet, M.J. and Nelson, K.A., "Optical Generation and Characterization of Acoustic Waves in Thin Films: Fundamentals and Applications", *Ann. Rev. Mater. Sci.*, **30**, 117 (2000).
83. <https://www.semilab.hu/metrology/infrared-inspection/surfacewave%E2%84%A2>
84. Bescond, C., Kruger, S.E., Lévesque, D., Lima, R.S. and Marple, B.R., 'In-Situ Simultaneous Measurement of Thickness, Elastic Moduli and Density of Thermal Sprayed WC-Co Coatings by Laser-Ultrasonics', *J. Thermal Spray Tech.*, vol.16, no 2 pp 238-244, (2007).
85. Monchalain, J.-P., "Progress towards the application of laser-ultrasonics in industry", in *Review of Progress in Quantitative Nondestructive Evaluation*, vol. 12, edited by D. O. Thompson and D. E. Chimenti, Plenum, New-York, 1993, p. 495, cited above.
86. Padioleau, C., Bouchard, P., Héon, R., Monchalain, J.-P., Chang, F. H., Drake, T. E. and McRae, K. I., "Laser ultrasonic inspection of graphite epoxy laminates", in *Review of Progress in Quantitative Nondestructive Evaluation*, Vol., 12, eds. D. O. Thompson and D. E. Chimenti, Plenum, New-York, 1993), p. 1345.
87. Chang, F. H., Drake, T. E., Osterkamp, M. A., Prowant, R. S., Monchalain, J.-P., Héon, R., Bouchard, P., Padioleau, C., Froom, D. A., Frazier, W. and Barton, J. P., "Laser ultrasonic inspection of honeycomb aircraft structures" in *Review of Progress in Quantitative Nondestructive Evaluation*, vol. 12, eds. D. O. Thompson and D. E. Chimenti, Plenum, New-York, 1993, p. 611.
88. Drake Jr, T. E., "Review of LaserUT™ Production Implementation", presented at *Review of Progress in Quantitative Nondestructive Evaluation*, Green Bay, Wisconsin, July 27-August 1, 2003, unpublished.
89. Drake Jr, T. E., Dubois, M., Osterkamp, M., Yawn, K., Tho Do, Kaiser, D., Maestas, J. and Thomas, M., "Review of Progress of the LaserUT™ Technology at Lockheed Martin Aeronautics Company", presented at *Review of Progress in Quantitative Nondestructive Evaluation*, Brunswick, Maine, July 31- August 5, 2005, unpublished.
90. Fiedler, C. J., Ducharme, T., Kwan, J., "The laser-ultrasonic inspection system (LUIS) at The Sacramento Air Logistics Center", *Review of Progress in Quantitative Nondestructive Evaluation*, vol.16, eds. Thompson D. O. and Chimenti D. E., Plenum, New-York, 1997, vol.16, p. 515.
91. Nelson, J. M., Nerenberg, R. L., Rempt, R. D., Shepherd, W. B., Sorsher, S. M., Woodmansee, W. E., Choquet, M., Monchalain, J.-P., "Enhanced laser generated ultrasound", Contract F33615-96-C-5268, Final report to the US Air Force, D950-10322-1, The Boeing Information, Space and Defense Systems, Seattle, 8 July 1998.
92. Pétilion, O., Dupuis, J.-P., Voillaume, H., Trétout, H., "Applications of Laser Based Ultrasonics to Aerospace Industry", *Proceedings of the 7th European Conference on Non-Destructive Testing*, Copenhagen, 26-29 May 1998, p.27.
93. Esmeralda Cuevas Aguado, E., Cabellos, E., Rubio Garcia, L., 'Laser Ultrasonics Inspections of Aeronautical Components with High Cadence and Geometrical Variations, Manufactured by RTM: Resin Transfer Moulding', *6th International Symposium on NDT in Aerospace*, 12-14th November 2014, Madrid, Spain.
94. <http://www.tecnatom.es/en/news/tecnalus-laser-technology-for-the-aeronautical-sector>
95. Blouin, A., Padioleau, C., Néron, C. and Monchalain, J.-P., 'A Laser-Ultrasonic System for the Inspection of Large Structures Fabricated by Automatic Fiber Placement', *Review of Progress in Quantitative Nondestructive Evaluation*, Burlington, Vermont, July 2011, vol. 30, AIP Conference Proceedings, vol. 31, American Institute of Physics, Melville, NY (2012).
96. Néron, C., Padioleau, C., Blouin, A. and Monchalain, J.-P., 'Robotic Laser-Ultrasonic Inspection of Composites', *Review of Progress in Quantitative Nondestructive Evaluation*, Denver CO, July 2012, AIP Conference Proceedings, vol. 31, American Institute of Physics, Melville, NY (2013).

97. Monchalain, J.-P., Néron, C., Bussière, J.F., Bouchard, P., Padioleau, C., Héon, R., Choquet, M., Aussel, J.-D., Carnois, C., Roy, P., Durou, G., Nilson, J.A., "Laser-ultrasonics: from the laboratory to the shop floor", *Advanced Performance Materials*, **5**, 7 (1998).
98. Choquet, M., Héon R., Padioleau C., Bouchard P., Néron C. and Monchalain, J.-P., "Laser ultrasonic inspection of the composite structure of an aircraft in a maintenance hangar", *Review of Progress in Quantitative Nondestructive Evaluation*, vol. 14, eds. D. O. Thompson and D. E. Chimenti, Plenum, New-York, 1995, p. 545.
99. Ochiai, M., Lévesque, D., Talbot, R., Blouin, A., Fukumoto, A. and Monchalain, J.-P., "Visualization of surface-breaking tight cracks by laser-ultrasonic F-SAFT", in *Review of Progress in Quantitative Nondestructive Evaluation*, vol. 22A, eds. D. O. Thompson and D. E. Chimenti, AIP Conference Proceedings, New-York, 2003, p. 1497.
100. Levesque, D., Dubourg, L. and Blouin, A., 'Laser ultrasonics for defect detection and residual stress measurement of friction stir welds', *Nondestructive Testing and Evaluation*, **26**, pp 319–333 (2011).
101. Mandache, C., Levesque, D., Dubourg, L. and Gougeon, P., 'Non-destructive detection of lack of penetration defects in friction stir welds', *Science and Technology of Welding and Joining*, **17**, pp 295-303, (2012).
102. Yamamoto, S., Hoshi, T., Miura, T., Semboshi, J., Ochiai, M., Fujita, Y., Ogawa, T. and Asai, S., 'Defect Detection in Thick Weld Structure Using Welding In-Process Laser Ultrasonic Testing System', *Materials Transactions*, **55**, pp. 998-1002, (2014).
103. Lévesque, D., Asami, Y., Lord, M., Bescond, C., Hatanaka, H., Tagami, M. and Monchalain, J.-P., 'Inspection of thick welded joints using laser-ultrasonic SAFT', *Ultrasonics*, **69**, pp 236-242 (2016).
104. Kruger, S. E., Lord, M. and Monchalain J.-P., unpublished.
105. Levesque, D., Bescond, C., Lord, M., Cao, X., Wanjara, P. and Monchalain, J.-P., Inspection of Additive Manufactured Parts using Laser ultrasonics, *Review of Progress in Quantitative Nondestructive Evaluation*, Minneapolis, MN from July 25–31, 2015, AIP Conference Proceedings, vol. 34, American Institute of Physics, Melville, NY.
106. Everton, S., Dickens, P., Tuck, C. and Dutton, B., 'Evaluation of laser ultrasonic testing for inspection of metal additive Manufacturing', *Laser 3D Manufacturing II, Proc. of SPIE*, Vol. 9353, H. Helvajian, A. Piqué, M. Wegener, B. Gu, eds, SPIE 2015.
107. Dubois, M., Moreau, A., Militzer M. and Bussière, J. F., "A New Technique for the Quantitative Real-Time Monitoring of Austenite Grain Growth in Steel", *Scripta Materialia*, **42**, 867 (2000).
108. Lim, C.S., Kang, M.G., Park, H.C., Huh, H.G., Oh, K.J., Nagata, Y., Yamada, H., Hashiguchi, S., 'Measurement of Grain Size of Hot-rolled Steel Sheets using Laser-Based ultrasonics', *IFAC Workshop on Automation in the Mining, Mineral and Metal Industries*, Gifu, Japan, September 10-12, 2012.
109. <https://www.gleeble.com/products/laser-ultrasonic-measurement-system-lumet.html>
110. Dubois, M. et al, 'Laser-ultrasonic monitoring of phase transformations in steels', *Scripta Materialia*, **39**, pp.735-741, 1998.
111. Dubois, M., Moreau, A., Bussière, J.Y., 'Ultrasonic velocity measurements during phase transformations in steels using laser ultrasonics', *J. Appl. Physics*, **89**, no11, pp 6487-6495 (2001).
112. Lim, C.S., Park, H.C., Kang, M.G., Huh, H.G., 'Development of measurement technology of phase transformation ratio on steel plates using laser-ultrasound', *International Conference on Control Automation and Systems (ICCAS), 2010*.
113. Nagata, Y., Yamada, H., Hashiguchi, S., Lim, C.S., Kang, M.G., Park, H.C., Huh, H.G., Oh, K.J., 'Phase Transformation Ratio Measurement of Steel Sheets Using Laser-Based Ultrasonics', *IFAC Workshop on Automation in the Mining, Mineral and Metal Industries*, Gifu, Japan, September 10-12 2012
114. Jacques, P.J., S. Allain, O. Bouaziz, A. De, A.-F. Gourgues, B. M. Hance, Y. Houbaert, J. Huang, A. Iza-Mendia, S. E. Kruger, M. Radu, L. Samek, J. Speer, L. Zhao and S. van der Zwaag 'On measurement of retained austenite in multiphase TRIP steels -results of blind round robin test involving six different techniques', *Materials Science and Technology* (2009) vol.25, no 5, pp 567-574.
115. Kruger, S., Damm, E.B., 'Monitoring austenite decomposition by ultrasonic velocity', *Material Science and Engineering*, A **425** 238-243 (2006).
116. Lamouche, G., Kruger, S. E., Gille, G., Giguère, N., Bolognini S. and Moreau, A., "Laser-Ultrasonic Characterization of the Annealing Process of Low-Carbon Steel", in *Review of Progress in Quantitative Nondestructive Evaluation*, vol. 22B, eds. D. O. Thompson and D. E. Chimenti, AIP Conference Proceedings, New-York, 2003, p. 1681.
117. Lindh-Ulmgren, E., Ericsson, M., Artymowicz, D., Hutchinson, B., 'Laser-ultrasonics as a technique to study recrystallization and grain growth', *Mater Sci Forum* 467-470 (2004).

118. Moreau, A., Lévesque, D., Lord, M., Dubois, M., Monchalain, J.-P., Padioleau, C., Bussière, J.F., 'On-line measurement of texture, thickness and plastic strain ratio using laser-ultrasound resonance spectroscopy', *Ultrasonics*, **40**, pp 1047-1056 (2002).
119. Kruger, S. E., Moreau, A., Militzer M. and Biggs, T., "In-Situ, Laser-Ultrasonic Monitoring of the Recrystallization of Aluminum Alloys" *Thermec 2003 International Conference on Processing & Manufacturing of Advanced Materials*, Part 1. Eds. T. Chandra, J. M. Torralba and T. Sakai., Trans Tech Publications Ltd., Uetikon-Zurich, 2003, p. 483.
120. Moreau, A., Bescond, C., Bolognini, S., Lord, M., Kruger, S.E., 'In-line Measurements of Texture and Recrystallization at Commonwealth Aluminum Corporation, final report, 2003 (unpublished).
121. Moreau, A., Lord, M., Lévesque, D., Dubois, M., Bussière, J.F., Monchalain, J.-P., Padioleau, C., Lamouche, G., Veres, T., Viens, M., Hébert, H., Basséras, P., Jen, C.-K., 'On-line Nondestructive Mechanical Properties Measurements using Laser-Ultrasonography', Final Report American Iron and Steel Institute, 2001 (unpublished).
122. Legrand, N., Sarkar, S., Damoiselet, F., Satyanarayan, L., Peron, T., Nogues, M., Lévesque, D., Lord, M., Lefaudeux, N., Collet, J.-L., Naumann, N., 'Laser Ultrasonic Sensor to Monitor Steel Microstructure at Elevated Temperature: Application to Hot Rolling', *4th International Symposium on laser-ultrasonics and Advanced Sensing*, Evanston, IL, USA, June 29-July 2, 2015, proceedings, paper 53.
123. Yu, A. and Gupta, V., 'Measurement of in situ fiber/matrix interface strength in graphite/epoxy composites', *Composites Science and Technology*, **58**, pp. 1827-1837 (1998).
124. Boustie, M., Auroux, E. and Romain, J.-P., 'Application of the laser spallation technique to the measurement of the adhesion strength of tungsten carbide coatings on superalloy substrates', *Eur. Phys. J. AP* **12**, 47{53 (2000).
125. Bossi, R., Housen, K., Walters, C. T. and Sokol, D., 'Laser bond Testing', *Materials Evaluation*, **67**, pp 819-27 (2009).
126. Perton, M., Blouin, A. and Monchalain, J.-P., 'Adhesive bond testing of carbon-epoxy composites by laser shockwave', *J. Phys. D: Appl. Phys.* **44**, 034012, 12pp (2011).
127. <http://www.lspstechnologies.com/brochures/LBI%20brochure%202014%20reduced%20size.pdf>
128. Barker, L. M. and Hollenbach, R. E., 'Laser interferometry for measuring high velocities for any reflecting surface', *J. Appl. Phys.*, **43**, pp. 4669-75 (1972).
129. Arrigoni, M., Monchalain, J.-P., Blouin, A., Kruger, S.E. and Lord, M., 'Laser Doppler Interferometer based on a Solid Fabry-Perot Etalon for Measurement of Surface Velocity in Shock Experiments', *Measurement Science and Technology*, **20**, 015302, 2009, 7pp.
130. Perton, M., Lévesque, J.-P., Monchalain, M., Lord, J. A. Smith, B. H. Rabin. Laser Shockwave technique for Characterization of Nuclear Fuel Plate Interfaces, *Review of Progress in Quantitative Nondestructive Evaluation*, Denver, CO, July 2012, AIP Conference Proceedings, vol. 31, American Institute of Physics, Melville, NY (2013).
131. Monchalain, J.-P., Perton, M., Lévesque, D., Blouin, A., Lord, M., Rousseau, G., Cole, R., Adhesive Bond Testing between Composite Laminates by Laser Shockwave Loading, 19th Int. Conf. on Composite Materials, Montreal (2013).
132. Fomitchov, P. A., Kromine, A. K., Krishnaswamy, S. and Achenbach, J. D., "Ultrasonic imaging of small surface-breaking defects using scanning laser source technique", in *Review of Progress in Quantitative Nondestructive Evaluation*, vol. 21A, eds. D. O. Thompson and D. E. Chimenti, AIP Conference Proceedings, New-York, 2002, p. 356.
133. Choquet, M., Lévesque, D., Massabki, M., Néron, C., Bellinger, N.C., Forsyth, D., Chapman, C.E., Gould, R., Komorowski, J. P., Monchalain, J.-P., "Laser-ultrasonic detection of hidden corrosion in aircraft lap joints: results from corroded samples", in *Review of Progress in Quantitative Nondestructive Evaluation*, vol. 20A, eds. D. O. Thompson and D. E. Chimenti, AIP Conference Proceedings, New-York, 2001, p. 300.
134. Blouin, A., Reid, B., Monchalain, J.-P., "Laser-ultrasonic Measurements of the Elastic Properties of a Static and a Moving Paper Web and of the Web Tension", in *Review of Progress in Quantitative Nondestructive Evaluation*, vol. 20A, eds. D. O. Thompson and D. E. Chimenti, AIP Conference Proceedings, New-York, 2001, p.271.
135. Ridgway, P. L., Hunt, A. J., Quinby-Hunt, M., Russo, R. E., "Laser-ultrasonics on moving paper", *Ultrasonics*, **37**, 395 (1999).
136. Ridgway, P. L., Russo, R. E., Lafond, E.F., Jackson, T.G., Baum G.A., Zhang, X. "Laser Ultrasonic Measurement of Elastic Properties of Moving Paper: Mill Demonstration" in *Review of Progress in QNDE*, vol. 25, eds. D.O. Thompson and D.E. Chimenti, AIP Conference Proceedings, New-York, 2006, ?.
137. Choquet, M., Héon, R., Vaudreuil, G., Monchalain, J.-P., Padioleau, C., Goodman, R. H., "Remote Thickness Measurement of Oil Slicks on Water by Laser-Ultrasonics", Proceedings of the *1993 International Oil Spill Conference*, Tampa, Florida, March 29-April 1, 1993, American Petroleum Institute, Washington DC, publication # 4580, p. 531.
138. Néron, C., Padioleau, C., Monchalain, J.-P., Choquet, M., Brown, C.E., Fingas, M.F., "Laser Ultrasonic Measurement of the Thickness of Oil Spills from an Airplane", presented at the *Review of Progress in Quantitative Nondestructive Evaluation*, Brunswick, Maine, July 31- August 5, 2005, unpublished.

139. Howard, T., Erdahl, D., Ume, I. C., Gamalski, J., Achari, A., "Development of an advanced system for inspection of flip chip and chip scale package interconnects using laser ultrasound and interferometric techniques", 2002 International Conference on Advanced Packaging and Systems, *Proceedings of the SPIE*, vol. 4828, 2002, pp. 136-142.
140. Fujita, M., Kotyaev, O., Shimada, Y., Non-Destructive Remote Inspection for Heavy Constructions, CLEO Technical Digest, 2012, Optical Society of America.
141. Bescond, C., Lévesque, D., Lord, M., Monchalain, J-P. and Forgues, S., 'Laser-generated surface skimming longitudinal wave measurement of residual stress in shot peened samples', Review of Progress in QNDE, vol. 25, eds. D.O. Thompson and D.E. Chimenti, AIP Conference Proceedings, New-York, pp1426-1433, (2006)
142. Lord, M., Levesque, D., Blouin, A. and Monchalain, J-P., 'Laser-ultrasonics for non-contact determination of longitudinal stress in rails', *4th International Symposium on laser-ultrasonics and Advanced Sensing*, Evanston, IL, USA, June 29-July 2, 2015, paper 31 in proceedings.